FUNCTIONAL CHARACTERIZATION OF *FAM49B* IN T CELLS DURING *SALMONELLA* INFECTION

Jamie Kim

DEPARTMENT OF HUMAN GENETICS,
MCGILL UNIVERSITY, MONTREAL
APRIL 2020

A thesis submitted to McGill University in partial fulfillment of the requirements of the degree of Master of Science

ABSTRACT

Salmonellae are motile, Gram-negative bacteria commonly transmitted through the ingestion of contaminated food and water. They can infect a broad range of hosts causing diseases extending from typhoid fever to gastroenteritis. *Salmonella* Typhimurium infection in susceptible mice is a model for human systemic disease. Through a recessive *N*-ethyl-*N*-nitrosourea (ENU) mutagenesis screen for susceptibility to infection with *Salmonella* Typhimurium, followed by mapping and exome sequencing, *Family with sequence homology 49 member b* (*Fam49b*) was identified as a novel *Salmonella* susceptibility gene. We have recently shown that FAM49B expressed in myeloid cells play an important role in resistance to *Salmonella* infection. This project aims to investigate the potential role of *Fam49b* in T lymphocytes during *Salmonella* infection.

A T cell conditional knockout mouse model of *Fam49b* was generated and then challenged with *Salmonella* infection. *Fam49b* deletion in T cells minimally affected susceptibility to infection compared to littermate controls. Despite the lack of a major clinical phenotype, in the *Fam49b* T cell-specific conditional knockout mice there was a depletion in $CD8^+$ T cells at steady state, which was associated with elevated activation, increased cytokine production (IFN- γ and IL-13), and enhanced proliferative ability. No differences were found in cell death or thymocyte development to account for the decrease in $CD8^+$ T cells, suggesting that *Fam49b* either induces a homeostatic response or acts as a T cell activation modulator. Given its role as a cytoskeleton regulator and the significance in myeloid cell mechanisms, *Fam49b* has a promising role in T cell activity and future experiments are needed to explore this possibility.

RÉSUMÉ

Les salmonelles sont des bactéries mobiles à Gram négatif communément transmises par l'ingestion d'aliments et d'eau contaminés. Elles ont la capacité de provoquer un large spectre de symptômes chez l'homme et chez les animaux, allant d'un portage asymptomatique à une infection généralisée (sepsis) pouvant être fatale. L'infection à *Salmonella* Typhimurium chez les souris sensibles est un modèle de maladie systémique humaine. Grâce à la mise en place d'une approche basée sur un crible de mutagenèse à l'éthyl-nitroso-urée (ENU) avec pour objectif d'identifier de nouveaux gènes impliqués dans la sensibilité à l'infection par *Salmonella* Typhimurium, le gène *Fam49b* (Family with Sequence Similarity 49 Member B) a été identifié comme un nouveau gène de sensibilité à la salmonelle. Nous avons récemment démontré que FAM49B exprimé dans les cellules myéloïdes joue un rôle important dans la résistance à l'infection à *Salmonella*. Ce projet vise à étudier le rôle potentiel de FAM49B dans les lymphocytes T lors d'infection à *Salmonella*.

Un modèle de souris knockout conditionnel où l'expression de *Fam49b* est spécifiquement supprimée dans les cellules T a été développé. Nous avons démontré que la délétion de *Fam49b* dans les cellules T a très peu affecté la susceptibilité à l'infection à *Salmonella*. Toutefois, nous avons observé que le nombre de lymphocytes T $CD8^+$ étaient diminué chez les souris invalidée pour le gène *Fam49b* dans les lymphocytes T. Cette diminution est observée à l'état d'équilibre et était associée à un phénotype d'activation élevée, une production accrue de cytokines (IFN-γ et IL-13) et une capacité de prolifération augmentée. Afin de déterminer pourquoi les lymphocytes T étaient moins abondants chez les souris *Fam49b* knock-out que chez les souris contrôles, certains aspects mécanistiques ont été étudiés. Tout d'abord nous avons vérifié différents processus de mort cellulaire et la maturation des lymphocytes dans le thymus. Nous n'avons pas observé de différences significatives dans la mort cellulaire ou le développement des thymocytes qui

pourraient expliquer la diminution des lymphocytes T $CD8^+$ chez les souris *Fam49b* knock-out. Ces résultats suggèrent que FAM49B induit soit une réponse homéostatique ou agit comme modulateur d'activation des lymphocytes T.

Compte tenu de son rôle de régulateur du cytosquelette et de son importance dans l'interaction complexe hôte-pathogène, FAM49B joue certainement un rôle important dans la fonction de plusieurs types cellulaires. Il sera donc nécessaire de poursuivre les travaux de recherche pour tracer un portrait complet du rôle de FAM49B dans l'activité des lymphocytes T dans un contexte de santé et de maladie.

TABLE OF CONTENTS

LIST OF ABBREVIATIONS

APC	Antigen-presenting cells
BMDMs	Bone marrow-derived macrophages
CDC42	Cell division control protein 42
CFSE	Carboxyfluorescein succinimidyl ester
CFU	Colony Forming Unit
CM	Central Memory
CTL	Cytotoxic T lymphocyte
CYFIP	Cytoplasmic FMR1 Interacting Protein 1
DNA	Deoxyribonucleic acid
DUF1394	Domain of Unknown Function 1394
ENU	*N*-ethyl-*N*-nitrosourea
ERAAP	Endoplasmic reticulum aminopeptidase associated with antigen processing
FAM49	Family with Sequence Similarity 49
Fam49b	Family with Sequence Similarity 49 Member B
FL9	FYAETPML
HIV	Human immunodeficiency virus
IFN	Interferon
IL	Interleukin
iNTS	Invasive non-typhoidal *Salmonella*
Ity15	*Immunity to Typhimurium locus* 15
LCMV	Lymphocytic choriomeningitis virus
LIP	Lymphopenia induced proliferation

LPS	Lipopolysaccharide
M cell	Microfold cell
MAP	Mitogen-activated protein
MHC	Major histocompatibility complex
N-WASP	Neural Wiskott-Aldrich syndrome protein
NF-κβ	Nuclear factor κβ
NTS	Non-typhoidal *Salmonella*
PBS	Phosphate-buffered-saline
PCR	Polymerase chain reaction
PDAC	Pancreatic ductal adenocarcinoma
PMA	Phorbol 12-myristate 13-acetate
pMHCI	Peptide MHC class I
PMN	Polymorphonuclear
PS	Phosphatidylserine
RAC1	Ras-related C3 botulinum toxin substrate 1
RNS	Reactive nitrogen species
ROS	Reactive oxygen species
SCV	*Salmonella* containing vacuoles
Sip	Salmonella invasion protein
Slc11a1	*Solute carrier family 11 member*
SPI	*Salmonella* Pathogenicity Islands
T3SS	Type III secretory system
TCR	T cell receptor

TNF	Tumour necrosis factor
TSB	Tryptic soy broth
WRC	WAVE regulatory complex

LIST OF FIGURES

CHAPTER 1:

CHAPTER 3:

LIST OF TABLES

ACKNOWLEDGEMENTS

McGill University resides on the traditional and unceded land of the Kanien'kehà:ka, a place which has long served as a site of meeting and exchange amongst nations. I would like to recognize and respect the Kanien'kehà:ka as the traditional custodians of the lands and waters on which we conduct research and study today.

I would like to express my deepest gratitude to my supervisor, Dr. Danielle Malo, for allowing me to be in your lab. You have provided guidance and an immensely supportive environment throughout my degree. I have developed a great appreciation for fundamental science research and look forward to bringing the skills you have taught me into my career. I hope one day I can be as supportive of a mentor to others. I would also like to thank my supervisory committee: Dr. Silvia Vidal and Dr. Judith Mandl, for their time and insights.

Thank you to all past members of the Malo Lab: Line Larivière, Alanna Crouse, Megan Eva, and Megan Teh. You all are greatly missed. In particular, thank you to Megan Eva for her much needed guidance in the early stages of my project. A special thank you to Line, you have provided me with invaluable wisdom and expertise, I do miss your stories and laugh filling our halls. And thank you to Patricia D'Arcy for performing harvests as well as every infection.

A huge shout out to my friends, especially to my fellow graduate students, who have given me so much through their insight, solidarity, love and support. Research can present with many obstacles, but what I will remember is the memories clowning together.

Lastly, thank you to my parents and my sister who have always supported me in everything I pursue. To my Mom and Dad, I don't think I can ever thank you enough for all your sacrifices and hard work to provide for me and Alison. I hope I can continue to make the most of these opportunities and make you proud.

FORMAT OF THESIS

This thesis has been prepared following the guidelines provided by the Department of Graduate and Postdoctoral Studies at McGill University, and is presented as a traditional thesis. The study presented herein consists of the characterization of an actin modulator in T lymphocytes during *Salmonella* challenge.

CONTRIBUTIONS OF WORK

Initial immunophenotyping of B6.*Lck*-Cre(*Fam49b*$^{fl/-}$) mice was completed by Megan Eva. Genotyping protocols were developed and tested by Etienne Flammant. Technical assistance, including genotyping mice, was provided by Line Larivière. Mouse colony maintenance and infections were performed by Patricia D'Arcy. Dr. Judith Mandl generously provided *Tcrb*$^{-/-}$ and CD45.1 B6 mice. All hematology parameters were done at the McGill University's Diagnostic Laboratory Services of the Comparative Medicine and Animal Resources Centre. I, under the supervision of Dr. Danielle Malo, have performed and analyzed all other tasks and experiments described in this thesis.

CHAPTER 1: INTRODUCTION & LITERATURE REVIEW

1.1 *Salmonella* Classification

Salmonellae are motile bacteria commonly transmitted through the ingestion of contaminated food and water, which is a leading cause of food-borne illnesses. Their prevalence in the food chain has an immense global effect on economic and health systems. Environmental circumstances, the health status of the host, and virulence factors contribute to the burden of foodborne infectious diseases (1).

Salmonella, found within the Enterobacteriaceae family, is made up of facultative, rod-shaped, Gram-negative bacteria that is comprised of two species: *Salmonella enterica* and *Salmonella bongori*. *S. enterica* consists of six subspecies: *arizonae*, *diarizonae*, *enterica, houtenae*, *indica,* and *salamae*. *S. enterica* contains over 2,600 serovars, with human disease most commonly being associated with serovars within the subspecies *enterica*, including *Salmonella* Typhi and *Salmonella* Typhimurium (2). To try to organize the diversity of *Salmonella*, the Kauffman-White classification system was developed based on surface antigens: O (somatic), H (flagellar) and K (capsular) (3). Few serovars are host restricted and only can only infect a single host; for example, *Salmonella* Typhi is restricted to humans (4). Other serovars are promiscuous and zoonotic, such as *Salmonella* Typhimurium which can infect multiple hosts including humans.

1.2 *Salmonella* Epidemiology

Typically, *Salmonella* infection begins following the ingestion of contaminated food or water. Given the diversity in *Salmonella* serovars, salmonellosis includes several possible clinical syndromes including enteric fever, non-typhoidal *Salmonella* (NTS) gastroenteritis, and invasive non-typhoidal *Salmonella* (iNTS) infection.

1.2.1 Enteric Fever

Enteric fever, which includes typhoid and paratyphoid fever, is a systemic febrile disease of the reticuloendothelial system that can potentially be fatal. Typhoid fever is caused by *S.* Typhi and paratyphoid fever is caused by *S.* Paratyphoid A, B, and C. These serovars are restricted to humans and higher primate hosts and have not been found to infect other animal species. With a fecal-oral route of infection, *Salmonella*-associated disease states disproportionately affect areas with limited access to proper sanitation and clean water. Globally, there are an estimated 21.7 million new cases and 210,000 deaths attributed to typhoid fever every year (5,6). However, almost all cases are found in developing countries and nearly 80% of cases recorded in developed countries have been related to international travel (7, 8).

Following an incubation period of approximately 14 days, symptoms such as fever, fatigue, and headache can be observed (9). Symptoms can last several weeks without treatment but can resolve within a few days if treated with antimicrobial therapy. Complications can arise following an episode of enteric fever, such as intestinal perforation (10). The fatality rate of typhoid fever when untreated versus treated can go from 20% down to 1% (11). However, the emergence of multidrug-resistant *Salmonella* strains has now required second-line antimicrobial therapies for an effective remedy.

Chronic carriage can occur after recovery from acute febrile illness. 1-5% of those infected will continue to shed bacteria for up to several years in stool and urine (12). Approximately 25% of chronic carriers do not experience any clinical symptoms during infection (9). It has been found that the gall bladder may act as a reservoir for bacteria, with a correlation of chronic infection of *Salmonella* with gallstones, and in particular biofilm formation on gallstones (13,14). Prolonged treatment with high-dose antibiotics resolves most cases of long term infection (15). This ability

for the bacteria to linger within asymptomatic hosts may be a key factor in the persistence of *Salmonella* infection within the human population.

1.2.2 Gastroenteritis

In the developed world, *Salmonella* is typically associated with a food-borne disease, which results in gastroenteritis with symptoms such as nausea, vomiting, diarrhea, and abdominal pain. Non-typhoidal *Salmonella* serovars often associated with this diarrhoeal disease are *S.* Typhimurium and *S.* Enteritidis (16). These tend to be zoonotic with the ingestion of infected food animals or contaminated fresh produce being linked to the majority of *Salmonella*-related gastroenteritis (17). Every year, approximately 93.8 million cases and 155,000 deaths are attributed to non-typhoidal *Salmonella* (18). Generally, the infection resolves in less than 7 days without treatment, but treatment through anti-emetics, analgesia, or fluid replacement can provide much-needed symptom relief.

1.2.3 Invasive non-Typhoidal Salmonella (iNTS) Infection

In immunocompetent individuals, NTS infection is usually self-limiting and localized to the gastrointestinal system. In the context of immunosuppression, NTS infection can result in systemic bacteremia called iNTS (19) with more severe clinical manifestations. Presentation is similar to enteric fever with symptoms including chills, myalgia, and general malaise (20). The ability of some serovars to establish extra-intestinal infection in immunocompromised hosts has resulted in an annual 3.4 million cases and 680,000 deaths (21). In particular, individuals with advanced human immunodeficiency virus (HIV), mainly in sub-Saharan Africa, succumb to iNTS at a fatality rate of 70% compared to the overall fatality rate of 20% in HIV negative patients (22).

Some other high-risk factors include malaria, malnutrition, and anemia, affecting children to a greater degree (22, 23). In developed nations, cases of iNTS are infrequent, but are found in the context of defects in both the adaptive or innate immune system, such as HIV infection, autoimmune diseases, or primary immunodeficiencies (24).

1.3 *Salmonella* Pathogenesis

Infection begins when *Salmonellae* enter the host through the consumption of contaminated food or water. Once ingested, the majority of the bacteria will be destroyed by the acidic environment of the stomach, but some can withstand the low pH and migrate to the intestine (Figure 1.1) (25). *Salmonellae* will colonize the lumen of the small intestine through adherence to enterocytes (26). This results in the penetration of host epithelial cells with preferential invasion of microfold (M) cells overlying Peyer's patches (27, 28). *Salmonellae* will also be engulfed by $CD18^{+}$ phagocytes, which reach into the intestinal lumen between tight junctions (29, 30). Additionally, through certain virulence factors, bacteria can disrupt tight junctions and can also invade through this route (31). The bacteria will then have access to the gut-associated lymphoid tissue (GALT) where they are further internalized by professional phagocytes such as macrophages, neutrophils, and dendritic cells in an attempt to eliminate the bacteria (32).

Pathogens have a multitude of methods to evade phagocytosis and spread infection (33). Notably, *Salmonella* benefit from entering host cells and replicating intracellularly in this protective niche; therefore, avoiding clearance by neutrophils and shielding bacteria from anti-microbial peptides (34). Detection of the internalized bacteria induces macrophage activation and an inflammatory caspase response. Caspase-1 activation can lead to cell death as well as additional pro-inflammatory cytokine production through IL-1β and IL-18. This leads to a large

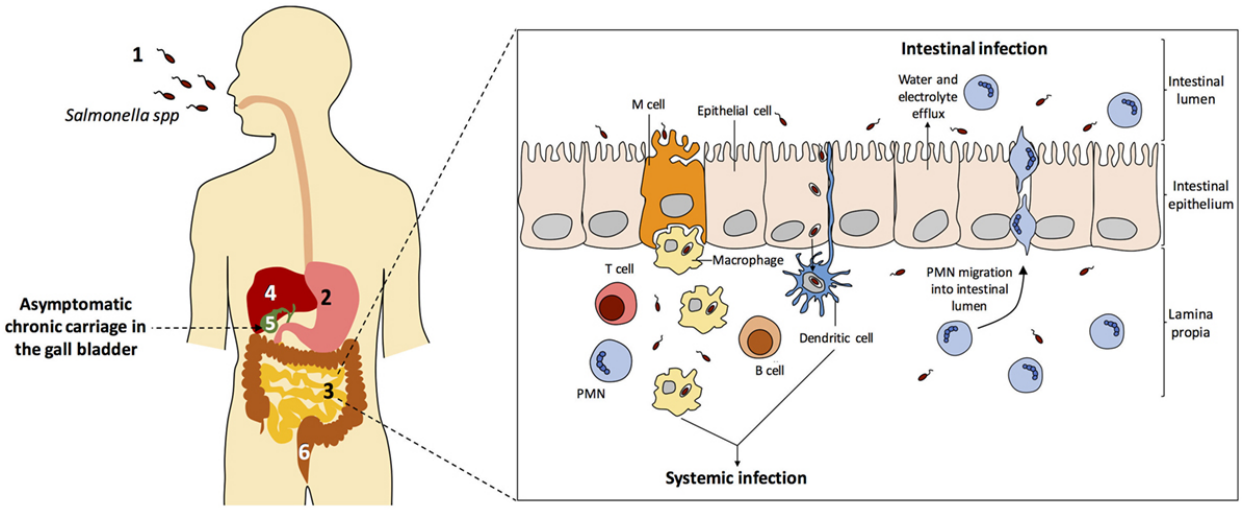

Figure 1.1: *Salmonella* Pathogenesis. *Salmonella* infection begins with the ingestion of contaminated food or water (1). Many of the bacteria will be killed by the low pH in the stomach (2). Some will colonize the intestine and invade epithelial cells such as microfold cells, enterocytes, or phagocytes (3). Through innate immune mechanisms, a massive influx of PMN cells to the area will be triggered in gastroenteritis. During systemic infection, the bacteria induce minimal intestinal inflammation and will be disseminated by macrophages, dendritic cells, and B cells to secondary tissues, such as the liver (4), spleen and lymph nodes. Bacteria can also infect the gall bladder, which has been identified as a likely reservoir for *Salmonella* in chronic carriage (5). These chronic carriers will shed the bacteria through feces for up to several years if left untreated (6). (Figure from (25) – open access article permitted for distribution)

influx of polymorphonuclear (PMN) cells and intestinal inflammation (35–38). NTS infection is then contained within the gastrointestinal system by this large recruitment of neutrophils and subsequent induction of diarrhea. Although NTS is limited to the intestines, immunocompromised individuals cannot elicit this massive immune cell response and the bacteria can disseminate to the bloodstream leading to invasive non-typhoidal *Salmonella*. *Salmonellae* then continue to persist

and replicate in protective *Salmonella* containing vacuoles (SCVs) within cells of secondary tissues, such as the spleen, liver, and lymph nodes (39). During enteric fever, *S.* Typhi and *S.* Paratyphi have altered virulence genes, which induces very minimal intestinal inflammation and neutrophil infiltration, allowing the bacteria to evade host defence mechanisms and spread the infection systemically (10, 40). With prolonged systemic infection, induction of the adaptive immune response results in a Th1 response with production of interferon-γ (IFN-γ) and tumour necrosis factor-α (TNF-α) (35, 36). This T cell response is needed for the complete resolution of infection (41, 42).

1.4 *Salmonella* Virulence Factors

Salmonella virulence is determined by genes crucial for invasion and survival, which requires organized timing and coordination. These genes are encoded in *Salmonella* Pathogenicity Islands (SPIs), with a total of 21 SPIs identified (43) – the most well-described being SPI-1 and SPI-2. Both encode type III secretory systems (T3SSs), which are essential for the virulence as mutations in several of these genes cause virulence attenuation. *Salmonella* uses T3SSs to inject effector proteins into host cells and exploit host cell mechanisms for their survival and replication (44). Type III secretory systems target host cells at multiple levels, including cytoskeleton modulation, vesicle trafficking, cytokine production, and cell death. Each gene seems to have varying effects on different cell types and it is believed that *S.* Typhi lacks many of the effector proteins specifically involved in a gastrointestinal inflammation (45).

1.4.1 SPI-1 Genes

Salmonella Pathogenicity Island 1 is associated with invasion of non-phagocytic cells, such as enterocytes and M cells of the intestinal epithelium (Figure 1.2) (45). Many SPI-1 genes encode effector proteins that are involved in actin modulation through activation of host Cell division control protein 42 (CDC42) and Ras-related C3 botulinum toxin substrate 1 (RAC1) signalling (46–48). This leads to actin polymerization through downstream neural Wiskott-Aldrich syndrome protein (N-WASP) and WAVE regulatory complex (WRC) activity. *Salmonella* invasion proteins SipA and SipC both promote processes involved in actin filament assembly (49, 50) while SopB, SopE, and SopE2 act as effector proteins for CDC42 and RAC1 signalling. For example, SopE acts as a guanine nucleotide exchange factor (GEF) for RAC1 signalling (51). This increased activity of cytoskeleton remodelling facilitates membrane ruffling and micropinocytosis to promote *Salmonella* internalization. Following the invasion of a host cell, virulence factor SptP acts as a GTPase-activating protein (GAP) by antagonizing RAC1 and CDC42 signalling, thereby halting membrane ruffling (48). Many SPI-1 effectors act on Nuclear factor κβ (NF-κB) or mitogen-activated protein (MAP) cascades to both induce and inhibit an inflammatory response through IL-8 production throughout the course of infection (37, 45, 52). In addition, SP1-1 virulence genes such as SipB can promote caspase-1 activation, which can then activate a greater inflammatory response with IL-1β and IL-18 production (53).

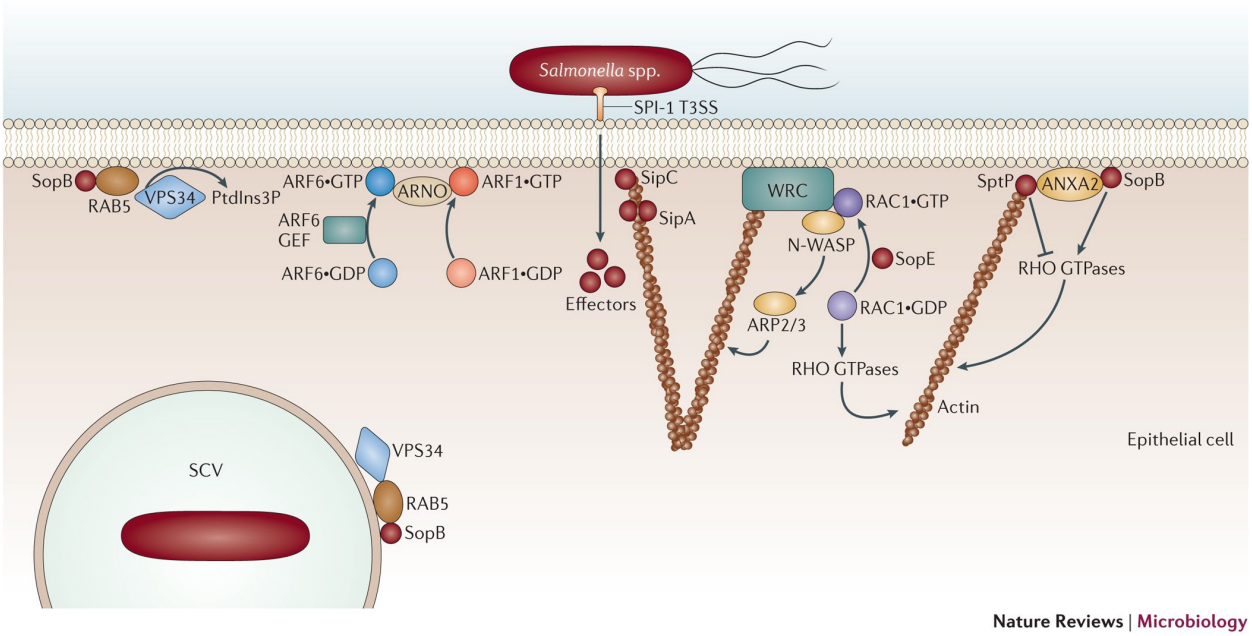

Figure 1.2: SPI-1 interactions during host cell invasion. *Salmonella* injects several virulence factors into host cells to promote internalization. SPI-1 effector proteins (in red) interact with multiple host processes to exploit actin modulation, such as RAC1 and CDC42 (RHO GTPase) activation. This leads to increased membrane ruffling and micropinocytosis. (Figure reproduced and reprinted with permission from (45))

1.4.2 SPI-2 Genes

Salmonella Pathogenicity Island 2 is associated with bacterial proliferation, particularly in response to acidification of SCVs (54, 55). Once inside the cells, *Salmonella* promotes the development of the SCV, which is important for bacterial survival. Both SPI-1 and SPI-2 genes coordinate for SCV development (56). The effector proteins work together to modulate maturation and trafficking of the SCV and to prevent fusion with lysosomes and further acidification (57). *Salmonella* Pathogenicity Island 2 genes are also responsible for the deterrence of reactive oxygen species (ROS) and reactive nitrogen species (RNS) to the SCV to avoid possible destruction of

bacteria and promote bacterial survival (58, 59). Many other SPI-2 genes are involved in furthering replication within host cells and aid in juxtanuclear positioning of the SCV for optimal bacterial replication (60, 61). Furthermore, SPI-2 has been found to have a role in suppressing immune cascades such as NF-κB and MAP kinase signalling (62, 63).

1.5 Host Response against *Salmonella*

The strategic mechanisms *Salmonella* utilizes to evade and hijack the host immune response are complex and not yet fully understood. Much of the genetic regulation involved in disease pathology is conserved between mouse and human. Although the murine system does not perfectly correlate with the human immune response, the use of murine models of *Salmonella* Typhimurium infection has been extremely helpful in unravelling the underlying genetics and mechanisms of infection susceptibility. Many factors can alter clinical outcome including serovar, infective dose, host genetics, and gut flora – all of which can be manipulated within the mouse model. Through studies of mouse models of infection, numerous novel genes and pathways central to the immune response against bacteria have been identified.

In modelling gastroenteritis, pre-treatment of mice with streptomycin disrupts the intestinal microbiota and the course of *S.* Typhimurium oral infection resembles salmonellosis-like disease in mice (64). In modelling enteric fever, serotypes *S.* Typhi and *S.* Paratyphi are restricted to humans and do not infect mice. There have been attempts to infect humanized mice with these serovars (65); however, these models do not replicate many aspects of human typhoid fever. *S.* Typhimurium is a natural pathogen of mice and systemic or oral infection of mice with *S.* Typhimurium models the disease progression of iNTS or typhoid fever in humans.

The genetic background of mice can drastically affect the response to infection, whether that be survival time or bacterial load. For example, 129 substrains are extremely resistant, compared to C57BL/6J which are extremely susceptible (66, 67). Solute carrier family 11 member (*Slc11a1*) is pleiotropic and has been described to be involved at multiple levels in the host response to intracellular pathogens, including *Salmonella* (68). C57BL/6J mice carry the mutant allele Gly^{169} of *Slc11a1,* which makes them exceedingly vulnerable (69). Upon challenge with *Salmonella*, *Slc11a1* is crucial for protection and is involved in controlling bacterial load, macrophage activation, pro-inflammatory cytokine responses, ROS and RNS production, and antigen presentation (69–72).

1.5.1 First Phase

The course of *Salmonella* infection can be divided into four phases (73). During the first phase of infection, the bacteria have crossed the epithelium and begins disseminating to secondary organs such as lymph nodes, spleen and liver. It is characterized by the rapid killing and clearance of *Salmonella* by phagocytes, such as neutrophils and macrophages. Pathogens are killed through the production of ROS and humoral immunity, such as antibodies and the complement cascade. Bacteria can be opsonized through complement C3b, a signal for phagocytosis. After cleavage of C5 into C5a and C5b, C5a then acts as a chemokine to bring neutrophils to clear the pathogen (74). C5b in coordination with C6, C7, C8, and C9 form the membrane attack complex (MAC), creating a transmembrane channel and leading to lysis of bacteria (75).

1.5.2 Second Phase (39)

The second phase of infection is defined by the exponential growth of *Salmonella* within cells and although bacteria killing persists, it becomes trivial. Bacteria is predominantly found in SCVs within resident phagocytes and dendritic cells from secondary lymphoid organs such as the spleen and lymph nodes. Pathogen-associated molecular pattern molecules (PAMPs), such as lipopolysaccharide (LPS), are recognized by innate immune cells through their pattern recognition receptors such as Toll-like receptors (TLRs) and Nod-like receptors (NLRs). This induces enhanced production of both pro-inflammatory (TNF-α, IFN-γ, IL-1, IL-6) and anti-inflammatory (IL-4 and IL-10) cytokines. In addition to bacterial growth control through ROS and RNS, the host employs cell death of infected macrophages as a protection mechanism and to prevent further proliferation and dissemination.

The host response at this phase determines the clinical outcome of infection. Resistant mice can subdue the exponential growth through innate immune mechanisms such as macrophage activation, production of antimicrobial peptides, ROS, and pro-inflammatory cytokines. Susceptible mice are unable to contain the growth of *Salmonella* and the bacteria evade death leading to overwhelming replication and likely death.

1.5.3 Third Phase

The third phase of infection is marked by a plateau in bacterial growth as innate immune cells contain replication through bactericidal and bacteriostatic methods. This suppression of the rate of bacterial growth will provide much needed time to mount a sufficient adaptive immune response and complete clearance of infection. An important process is the formation of granulomas of infected tissues to limit spread to the reticuloendothelial system (42, 76).

1.5.4 Fourth Phase

The fourth phase of infection involves the induction of the adaptive immune response through T and B cell activity. Although the innate response can control the infection, the adaptive immune compartment is essential for a full recovery and also protects from subsequent infections. B cells develop the ability to generate antibodies specific to *Salmonella* antigens, such as LPS and other antigenic epitopes, which become important during potential secondary exposure to *Salmonella*. B cells are also crucial in antigen presentation to initiate the T cell response. Mice deficient in B cells are unable to develop sufficient adaptive immunity and immunized mice succumb to *Salmonella* during repeat challenge (77, 78). Interestingly, the HLA-DRB1 allele is associated with protection for typhoid fever (79, 80) and has been attributed to its role in antigen presentation to T cells.

Lymphocyte-deficient mice are susceptible to *Salmonella* infection and determined to be mediated mostly by $CD4^+$ and in part by $CD8^+$ T cells (81, 82). The T cell immune response has a Th1 bias and promotes enhanced production of Th1 cytokines such as IFN-γ and TNF-α. The $CD4^+$ T cell response also induces additional activation of PMN cells and antigen presentation. In particular, IFN-γ secreting T cells have been found to be critical in *Salmonella* elimination (83). $CD8^+$ T cells differentiate into cytotoxic T lymphocytes (CTLs) and are thought to support the immune response through the killing of infected macrophages. Enhanced $CD8^+$ T cell activity has been found to be associated with improved outcomes of typhoid fever in humans (84). It is through the adaptive immune response that the infection is completely cleared from the host system.

1.6 The Role of *Fam49b*

Family with sequence similarity 49 (FAM49) proteins are evolutionarily conserved across many phyla. In mammals, there are two members of the *Fam49* family, *Fam49a* and *Fam49b*, that share 80% sequence identity. High levels of FAM49B expression were detected in patients with relapsing multiple sclerosis (85), but otherwise until recently little was known about the function of *Fam49b*. Now several additional studies have begun to elucidate the potential role of *Fam49b* in a variety of contexts.

1.6.1 Fam49b Involvement in Immune Surveillance

In 2012, a study identified *Fam49b* playing a possible role in immune surveillance. Endoplasmic reticulum aminopeptidase associated with antigen processing (ERAAP) process peptides for presentation by major histocompatibility complex (MHC) class I molecules (86). The study found that disruption of ERAAP induced presentation of a peptide FYAETPML (FL9) on MHC class Ib molecule Qa-1^b (87). Of note, naïve mice immunized with ERAAP knockout cells produced antigen-experienced $CD8^+$ T cells specific for Qa-1^b-FL9. The FL9 peptide that induced antigenic activity was found to be encoded by *Fam49b*. It was suggested, given the ubiquitous expression of *Fam49b*, the presentation of Qa-1^b-FL9 is a conserved mechanism of immune-surveillance to detect ERAAP defects and pMHC class I (pMHCI) presentation abnormalities.

1.6.2 Fam49b in Cancer Tumorigenesis

An investigation in pancreatic ductal adenocarcinoma (PDAC) found *FAM49B* to be associated with mitochondrial fission and cancer progression (88). In PDAC biopsy samples stained for FAM49B expression, the lymph node invasion rate was much higher in patients with

tumours stained negative. Interestingly, in mouse studies FAM49B expression was silenced in PDAC by the tumour microenvironment. While in PDAC cell lines, knockdown of *FAM49B* showed enhanced proliferation, migration, and tumour growth when injected into immunocompromised mice. In this study, the suppression of *FAM49B* expression caused changes in mitochondrial morphology and was associated with mitochondrial fission and elevated ROS. Considering their findings, the study points to a possibility of *FAM49B* regulating metabolic and mitochondrial dynamics, which impacts cancer metastasis. This group hypothesized that the tumour microenvironment inhibited FAM49B expression, which has the consequence of inducing pro-tumoral ROS in PDAC mitochondria, leading to subsequent increases in proliferation and invasiveness of the PDAC cells. FAM49B also promoted gallbladder carcinoma cell proliferation and migration through its regulation by Taspase 1-PI3K/AKT pathway (89).

1.6.3 Fam49b in T cell Activation and RAC1 Mediation

More recently, a genome-wide CRISPR screen sought out regulators of T cell activation and identified *Fam49b* as a potential regulator (90). They used single-guide RNA (sgRNA) to target gene expression in Jurkat T cells and determined activation phenotypes through the sorting of $CD69^{high}$ vs. $CD69^{low}$ T cells. Of the positive and negative regulators identified, *Fam49b* was found to be a promising novel negative regulator. Following T cell stimulation in Jurkat T cells, *Fam49b* deficiency enhanced CD69 expression and was found to have more prolonged and elevated MAP kinase phosphorylation. These results suggest FAM49B inhibits T cell activation and subsequent signal transduction.

To further investigate the possible cellular mechanism, immunoprecipitation in combination with mass spectrometry was used to identify binding interactors. FAM49B was found

to interact with RAC1, with a higher affinity to active RAC1-GTP. FAM49B is comprised of a single Domain of Unknown Function 1394 (DUF1394) and this domain is shared with Cytoplasmic FMR1 Interacting Protein 1 (CYFIP). CYFIP1 is a component of the WRC, which interacts with RAC1 through its DUF1394 domain to promote actin polymerization (91). Using the HADDOCK server, putative conserved residues (R161, R165, N154, A192, P150) involved in RAC1-binding were identified and mutated in the corresponding site of *Fam49b*. Mutation R161D within this interaction interface abolished binding between FAM49B and RAC1. Also, mutations at these key residues (A192L, R165D, R161D, N154D, P150R) abrogated the T cell activation phenotype. This group also found that downstream pathways of RAC1, such as PAK phosphorylation and actin polymerization, were enhanced in *Fam49b* mutants. Overall, their model suggests that FAM49B directly binds to and sequesters active RAC1-GTP, resulting in a reduction in RAC1 downstream effects such as T cell signal transduction and likely cytoskeletal remodelling.

1.6.4 FAM49 in RAC1-Mediated Actin Dynamics

A subsequent study looking at *Fam49*, investigated its interaction with RAC1 and the effects of cell migration and polarization in *Dictyostelium* cells. Similar to the previous study, they found FAM49 binds active-RAC1 through the DUF1394 domain given its conserved structural similarity with CYFIP. Interestingly, they found unique N-terminal myristoylation on FAM49 suggesting plasma membrane localization. Knockout of *Fam49b* in mammalian cell lines changed cell morphology with increased circularity and these cells developed broader lamellipodia associated with elevated levels of WAVE2. *Fam49b*-deficient cells also display longer and less extensive lamellipodial actin dynamics, causing the cells to lose their polarized lumen, plasticity

to reorient and speed in cell migration. Together, it seems FAM49 obstructs RAC1-Scar/WAVE mediated lamellipodia protrusions, suggesting that FAM49 plays a role in the feedback loop in regulating leading-edge actin dynamics.

Overall, *Fam49b* has been recently investigated in a variety of contexts through ERAAP processing for pMHCI presentation, PDAC tumorigenesis, T cell activation and actin dynamics in amoeba. Multiple studies have now identified *Fam49b* as a gene encoding an active-RAC1 interactor, which acts as a negative regulator for RAC1-mediated actin polymerization (90, 92, 93). Deletion of *Fam49b* in T cells induces elevated T cell activation *in vitro* (90); however, the mechanism of this is not fully understood. In *Dictyostelium* cells, *Fam49* suppresses lamellipodia protrusion formation and coordinated migration (92). In line with these observations, *Fam49b* deletion in PDAC was also shown to affect cell motility with *Fam49b*-deficient PDAC cell lines demonstrating enhanced migration (88). Although the PDAC study hypothesized that the increased tumorigenicity of FAM49B-negative PDAC was a consequence of elevated ROS, given the growing information of *FAM49B* function, it may indeed be due to the effects of uninhibited cytoskeleton remodelling. The discovery of the potential role of *Fam49b* in different cell types has painted an intriguing picture of the possible mechanisms and effects of *Fam49b.*

1.7 Role of FAM49B *in vivo*

A recent investigation completed by our group was done through a genome-wide recessive *N*-ethyl-*N*-nitrosourea (ENU) mutagenesis screen for susceptibility to infection with *S.* Typhimurium (93). Our lab identified several variant pedigrees including *Immunity to Typhimurium* locus 15 (*Ity15*). Mice from the *Ity15* pedigree exhibited increased susceptibility to

S. Typhimurium with a reduction in survival following systemic infection. *Ity15* mutant mice (*Ity15*$^{m/m}$) exhibited a higher bacterial load in the spleen, liver, and blood and had higher levels of pro-inflammatory cytokines (TNF-α and IL-6) and anti-inflammatory cytokines (IL-10) when compared to *Ity15*$^{+/+}$. In addition, *Ity15*$^{m/m}$ mice developed pathological changes associated with septicemia. Overall, this demonstrates the increased susceptibility to *S.* Typhimurium of *Ity15*$^{m/m}$.

To identify the causal gene, genome-wide linkage analysis was completed and mapped to a single linkage peak on chromosome 15. Next, exome sequencing found a T to A substitution within the splice donor site of exon 9 in *Fam49b*. This caused skipping of exon 9, a frameshift and a premature stop codon within exon 10, and abrogated expression of FAM49B in *Ity15*$^{m/m}$. Allelic complementation was done through a cross of *Ity15*$^{+/m}$ and *Fam49b*$^{+/-}$. *Ity15*^{m}/*Fam49b*$^{-}$ mice displayed increased susceptibility; therefore, displaying a lack of complementation. Collectively, this demonstrates the loss of *Fam49b* results in *Salmonella* susceptibility.

In parallel to the previously described studies, the structure of FAM49B was identified to include a single domain DUF1394 and was hypothesized to interact with RAC1 given its role in CYFIP1. *In vitro* assays showed the association of FAM49B with RAC1 and pull-down experiments using GST-RAC1 in the presence of GDP or GTP showed FAM49B preferentially binds to GTP-RAC1. Two predicted RAC1 binding sites within FAM49B were identified and concurrent mutations at both binding sites abolished RAC1 binding. This demonstrated FAM49B interacts with RAC1, similarly to CYFIP1 (93). This role of *Fam49b* has led to the recent renaming of the gene to CYFIP-related RAC1 interactor B (CYRIB).

Given the interaction of RAC1 with FAM49B and its involvement in actin polymerization, the role of FAM49B in cytoskeleton modulation was further explored. *Fam49b* knockout Hela cells were found to be round, unpolarized, and flattened – similar to the morphology of mutant

cells with ubiquitously activated RAC1. Also, these knockout cells displayed extensive ruffling and increased cellular spread and circularity compared to control cells. *Fam49b* deletion was also associated with enhanced actin polymerization. Therefore, *Fam49b* was shown to be a negative regulator of RAC1-driven actin cytoskeleton remodelling (93).

Cytoskeletal remodelling is important in two major processes in *Salmonella* dissemination: phagocytosis and cell migration. Given the importance of innate myeloid-derived phagocytes in *Salmonella* infection, the role of *Fam49b* was evaluated in the hematopoietic system. First, *Salmonella* resistance in the hematopoietic system was assessed through bone-marrow chimeras of $Ity15^{+/+}$ and $Ity15^{m/m}$ mice. Following the transfer of $Ity15^{+/+}$ bone marrow cells to $Ity15^{m/m}$ mice, enhanced resistance was conferred to the mutant mice. Conversely, following the transfer of $Ity15^{m/m}$ bone marrow cells to $Ity15^{+/+}$, increased susceptibility to *Salmonella* was observed. This shows the significance of the role of *Fam49b* in the hematopoietic system upon challenge with *Salmonella* (93).

To further study the role of *Fam49b* within the myeloid-derived phagocytes, a myeloid-specific conditional knockout mouse (B6.Tg(*Lysm*-Cre)$Fam49b^{-/flox}$) was generated. B6.Tg(*Lysm*-Cre)$Fam49b^{-/flox}$ mice succumbed to *Salmonella* infection faster than wild-type B6.Tg(*Lysm*-Cre)$Fam49b^{+/flox}$ mice. Furthermore, B6.Tg(*Lysm*-Cre)$Fam49b^{-/flox}$ mice displayed higher bacterial loads in the liver and spleen. This points to an important role of *Fam49b* in myeloid cells for protection against *Salmonella* infection (93).

Given this significance of *Fam49b* in myeloid-lineage cells in conferring resistance to *Salmonella*, macrophage phagocytosis and neutrophil migratory ability were then assessed. Bone marrow-derived macrophages (BMDMs) from B6.Tg(*Lysm*-Cre)$Fam49b^{+/flox}$ and B6.Tg(*Lysm*-Cre)$Fam49b^{-/flox}$ mice were infected with opsonized bacteria. B6.Tg(*Lysm*-Cre)$Fam49b^{-/flox}$

BMDMs had a higher percentage of *Salmonella* infected cells, demonstrating the role of *Fam49b* in controlling phagocytic potential. Next, neutrophils from B6.Tg(*Lysm*-Cre)*Fam49b*$^{+/flox}$ and B6.Tg(*Lysm*-Cre)*Fam49b*$^{-/flox}$ mice were evaluated for cell motility in a three-dimensional collagen matrix. The deletion of *Fam49b* in neutrophils significantly affected migratory behaviour, displaying higher velocities and more random migratory patterns. Both increased phagocytosis and altered cell migration may explain the increased bacterial dissemination seen in *Fam49b* deficiency. In concordance to this finding, a recent genome-wide CRISPR screen for phagocytosis identified *Fam49b* as a negative regulator of phagocytosis (93).

Through this study, our lab identified *Fam49b* as a RAC1 and cytoskeleton regulator in myeloid cells, which protects against *Salmonella* infection. *Fam49b* was involved in bacterial host cell invasion, phagocytosis, and subsequent dissemination (Figure 1.3) (93) not only during *Salmonella* infection but also infection with *Listeria monocytogenes* and *Mycobacterium tuberculosis*. Because of its important function in actin remodelling, a broader role for FAM49B within other immune cell types with associated implications in the host immune response is expected.

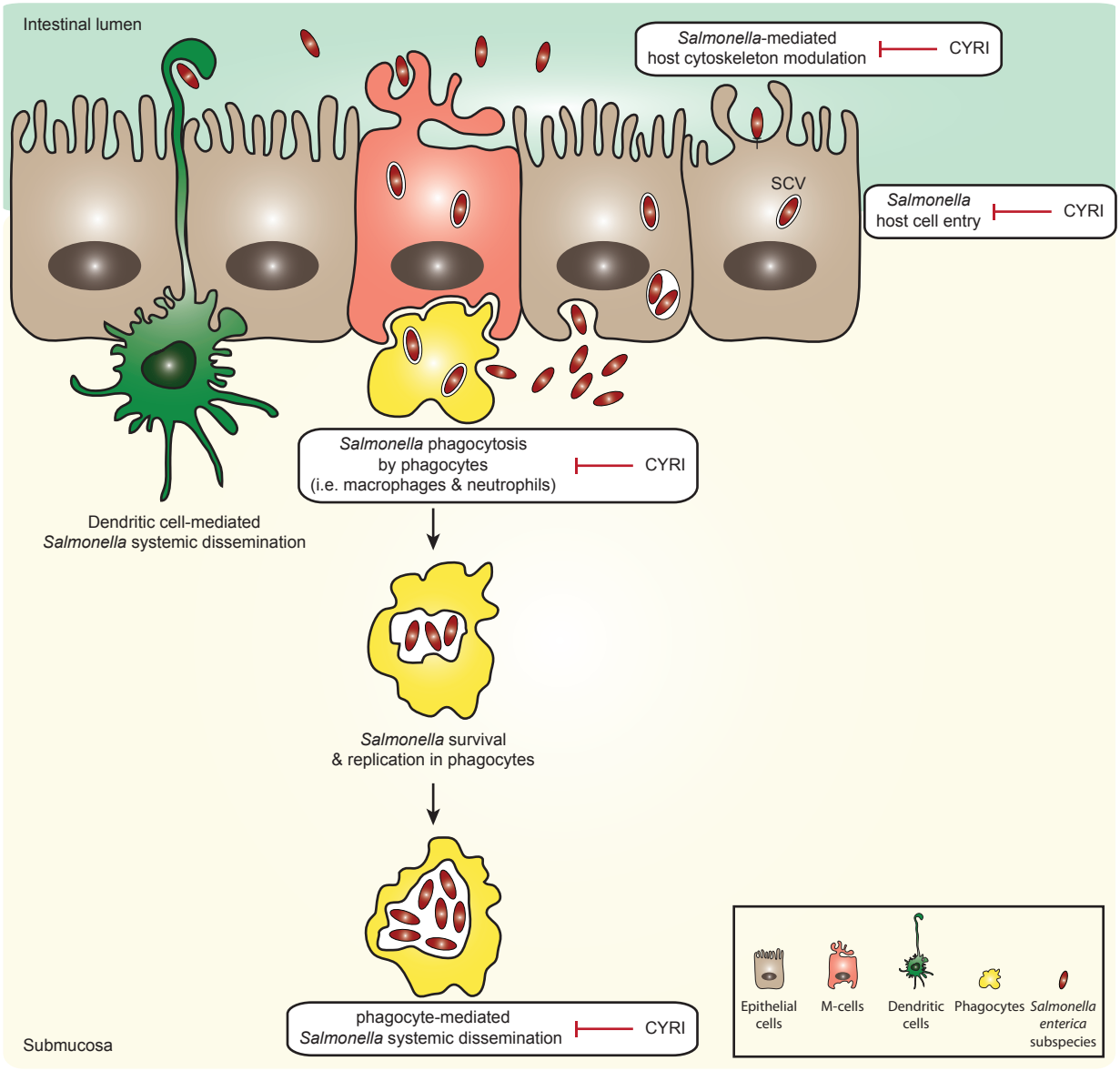

Figure 1.3: Model of FAM49B effect of *Salmonella* infection. Through its action as a RAC1 mediator, FAM49B was involved in bacterial host cell invasion, phagocytosis and subsequent dissemination. Its role affects multiple cell types at many points during the course of infection. (Figure reproduced and reprinted with permission from (93))

1.8 Project Hypothesis and Objectives

The burden of salmonellosis and other infectious diseases can be addressed with further understanding of the interplay between the host defence response and pathogen. Host genetics can elucidate the interconnected players involved in mounting a sufficient response for clearance and recovery from infection. This can be a difficult task with each genetic factor bearing several complex roles, but through using strategies such as forward genetics we have identified *Fam49b* as a novel gene implicated in susceptibility to *Salmonella* infection. Further characterization of its role in immunity will elucidate its significance in the host defence response.

Preliminary immunophenotyping found that *Ity15*$^{m/m}$ mice have depleted levels of CD8^{+} T lymphocytes with associated elevation in CD69 expression. This phenotype of T cell depletion and enhanced activation was not seen in the B6.Tg(*Lysm*-Cre)*Fam49b*$^{-/flox}$ mice, indicating a potential intrinsic role within T cells contributing to the phenotype. As mentioned previously, *Fam49b* deficiency was associated with a potential T cell activation phenotype *in vitro* (90) but has not yet been investigated *in vivo*. We **hypothesized** that *Fam49b* depletion induces a T cell activation phenotype through enhanced actin polymerization and may affect clinical outcomes to *Salmonella* infection. To address this, a lymphocyte-specific conditional knockout of *Fam49b* was generated. This mouse model was further characterized at steady-state as well as during *Salmonella* challenge. This project used microbiological techniques and flow cytometry to describe activation, cytokine production, cell death and proliferation of T cells within this model. The **objectives** of this project are to demonstrate the impact of *Fam49b* knockout in T cells, to determine its significance in the host defence response against *Salmonella* and elucidate further the function of *Fam49b*.

CHAPTER 2: MATERIALS & METHODS

Mice

All experiments were performed under guidelines specified by the Canadian Council for Animal Care. The animal-use protocol was approved by the McGill University Animal Care Committee (Protocol number 5797). C57BL/6J and B6.Cg-Tg(*Lck*-Cre)548Jxm/J mice were obtained from The Jackson Laboratory (Bar Harbor, ME, USA). C57BL/6N-*Fam49b*$^{tm1a(KOMP)Wtsi}$/Tcp (*Fam49b*^{tm1a}) mice were obtained from the NorCOMM Project. *Tcrb*$^{-/-}$ (B6.129P2-*Tcrb*^{tm1Mom}/J) and B6.SJL-CD45.1 (B6.SJL-*Ptprc*^{a} *Pepc*^{b}/BoyJ), originally from the Jackson Laboratory, were bred and maintained in the laboratory of Dr. Judith Mandl (McGill University). The *Fam49b*^{tm1a} KO-first allele was converted to a conditional allele (*Fam49b*^{tm1c}) through Flp recombination and the *Fam49b*$^{tm1c/tm1c}$ mice were crossed with Meox-Cre (B6.129S4-*Meox2*$^{tm1(cre)Sor}$/J) mice to generate the *Fam49b*^{tm1d} allele (Yuki et al 2019). B6.*Fam49b*$^{tm1c/tm1c}$, B6.*Fam49b*$^{tm1c/tm1d}$, B6.Tg(*Lck*-Cre)*Fam49b*$^{+/tm1d}$, B6.Tg(*Lck*-Cre)*Fam49*$^{tm1c/tm1c}$, *Tcrb*$^{-/-}$, B6.SJL-CD45.1, and C57BL/6J mice were maintained on a 12-hour light-dark cycle in the temperature-controlled facility of the McGill Goodman Cancer Centre with free access to food and water. Crosses were made between B6.Tg(*Lck*-Cre)*Fam49b*$^{+/tm1d}$ and B6.*Fam49b*$^{tm1c/tm1d}$ to generate control (B6.Tg(*Lck*-Cre)*Fam49b*$^{flox/+}$) and experimental (B6.Tg(*Lck*-Cre)*Fam49b*$^{flox/-}$) animals. Alternatively, crosses were made between B6.*Fam49b*$^{tm1c/tm1c}$ and B6.Tg(*Lck*-Cre)*Fam49b*$^{tm1c/tm1c}$ to generate control (B6.*Fam49*$^{+/+}$) and experimental (B6.Tg(*Lck*-Cre)*Fam49b*$^{flox/flox}$) animals. For *in vivo* and *ex vivo* experiments, either male or female mice aged between 7-16 weeks were included. Mice were age and sex-matched for each experiment.

Genotyping

Deoxyribonucleic acid (DNA) extractions were performed from mouse ear punches with digestion in lysis buffer and proteinase K overnight. Potassium acetate 8M was added, followed by chloroform. Samples were cooled at -20°C, spun in a centrifuge, and the top aqueous phase was placed in 100% ethanol. After a few hours at -80°C, the DNA precipitate was isolated through centrifugation and washed with 70% ethanol. DNA pellets were then air-dried for several minutes and resuspended in dH_2O. Genotyping was done using polymerase chain reaction (PCR) amplification and primers detailed in Table 1. *Fam49b* WT was used to identify the presence of the wild-type allele (857 bp band) and tm1c KO-first allele (1115 bp band). Intron 6-7 was used to discern which two of three *Fam49b* alleles (tm1c – 1821 bp band, wild-type – 1636 bp band, tm1d – 991 bp band) each mouse carried. Lck identified the presence of the transgene *Lck*-Cre recombinase (wild-type 324 bp band, tg *Lck*-Cre 250 bp band). Polymerase chain reaction products of *Fam49b* WT and Intron 6-7 were then run on agarose gels of 1.5%, while PCR products of Lck were run on 2.5% agarose gels.

***Salmonella* Stock Preparation and *in vivo Salmonella* Infection**

Salmonella Typhimurium strain SL1344 was used in all experiments. To prepare stock, one *Salmonella* colony was added to 4mL of tryptic soy broth (TSB), then placed on an oscillating wheel overnight at 37°C. The following day, 1mL of glycerol was added. Aliquots of *Salmonella* were kept frozen at -80°C. The day before the infection, 1000µL of frozen *Salmonella* stock was added to 25mL of TSB, then placed on a rotating shaker (200 rotations per minute) at 37°C until the mixture reached an optical density (measured at 600nm, OD_{600}) of approximately 1.0. The *Salmonella* culture was then placed on ice at 4°C for at least 2 hours. After the culture cooled, 1

in 10 serial dilutions were done with 10^{-4} and 10^{-5} dilutions plated on tryptic soy agar (TSA) plates. Plates were incubated overnight at 37°C and the culture of *Salmonella* was kept at 4°C overnight. The next day, colony-forming units (CFUs) were counted to calculate the concentration of *Salmonella*. *Salmonella* was diluted with 0.9% saline to achieve a concentration of 5 CFUs/µL. Mice were inoculated intravenously (i.v.) with 200µL of 1000 CFUs via the caudal vein. For survival analysis, mice were monitored twice a day for changes in mouse body score condition (94). Those individuals demonstrating a body condition score of less than 2 were humanely euthanized by exposure to CO_2. Spleens and livers were collected 5 days post-infection for CFU determination. Tissues were removed aseptically, weighed, placed in 3 mL of isotonic saline and homogenized using a tissue homogenizer (T25 Ultra-Turrax, IKA). The resulting homogenate was diluted in 1× Phosphate-buffered-saline (PBS) and serial dilutions were plated on tryptic soy agar to determine organ bacterial load. Spleen enlargement was measured using spleen index which is calculated by the following equation: $\sqrt{\frac{Spleen\ weight\ (g)\ /10}{Body\ weight\ (g)}}$

Hematology

Blood samples were collected by cardiac puncture into EDTA tubes (Sarstedt) for complete blood counts and white blood cell differential. Analyses were performed at the Comparative Medicine and Animal Resources Centre at McGill University. Data from females and males was pooled.

Cell Processing

Spleen, lymph node, and thymus were harvested under sterile conditions. Single-cell suspensions were prepared by processing the tissues through 70µm cell strainer (Fisherbrand). Red blood cells were lysed by treatment with Ammonium-chloride-potassium (ACK) buffer. Samples were then

washed with PBS and passed a second time through a cell strainer. Cells were counted using a hemocytometer and resuspended at a concentration of $20x10^6$/ml in complete RPMI and plated in 96-well microtitre plates (Falcon, BD Bioscience).

In vitro T cell Stimulation

For *in vitro* activation, T cells were stimulated with anti-CD3 (145-2C11, Invitrogen) and anti-CD28 (37.51, Invitrogen) or phorbol 12-myristate 13-acetate (PMA) and ionomycin. For the detection of intracellular cytokines, a cocktail of Brefeldin and Monesin (Invitrogen) was added 4-6 hours before the collection of cells. Cells were collected, washed and fixed using fixability/permeability solutions (BD Cytofix/Cytoperm). For proliferation analysis, T cells were exposed to anti-CD3 and anti-CD28 and were pre-loaded with 2.5μM carboxyfluorescein succinimidyl ester (CFSE) using the CellTrace CFSE Cell proliferation kit (Invitrogen) and cultured for 3-5 days. Interleukin-2 (IL-2) was added to the media on day 2.

Naïve T cells Enrichment and Adoptive Transfer

Naïve T cells were enriched using the EasySep™ Mouse Pan-Naïve T cells Isolation Kit (Stem Cell) by negative selection. Cells are targeted for removal using biotinylated antibodies directed against non-naïve T cells (CD11b, CD19, CD24, CD25, CD44, CD45R/B220, CD49b, TER119) and removed using streptavidin-coated magnetic particles. The purity of naïve T cells ($CD44^{lo}CD62L^{hi}$) was determined to be >92% by FACS analysis. For *in vitro* experiments, cells were cultures for 18 hours before fixation and staining. For *in vivo* experiments, *Tcrb*$^{-/-}$ mice received $6x10^6$ naïve T cells stained with 2.5μM of CFSE in 300μl sterile PBS by intravenous

injection. At day 7 post-transfer, spleen and lymph node lymphocytes were stained and analyzed through flow cytometry.

Flow Cytometry Analysis

Viability was evaluated using Zombi Aqua Fixable Viability Dye (Biolegend). To assess the thymus, cells were stained with CD44 BV711 (IM7, Biolegend), CD25 BV785 (PC61, Biolegend), CD4 PeCy7 (GK1.5, Invitrogen), CD8 APC (53-6.7, Biolegend). Splenocytes and lymph nodes were additionally stained with CD5 Alexa Fluor 700 (53-7.3, Biolegend), CD69 FITC (H1.2F3, Invitrogen) and CD62L BV421 (Biolegend). For intracellular staining, cells were permeabilized and stained with TNF-α PE (MP6-XT22, Biolgend), IL-17α BV605 (TC11-18, Biolegend), IFN-γ PerCP-Cyanine5.5 (XMG1.2, Invitrogen), IL-13 APC-eFluor 780 (eBio13A, Invitrogen), and IL-5 BV421 (TRFK5, Biolegend). Apoptosis was assessed using Annexin V FITC (eBioscience) and Fixable Viability Dye eFluor 780 (Biolegend). Samples were acquired using the FACS Fortessa and analyzed using FlowJo version 10.0.8r1. To assess cell death, lymphocytes were stained with Annexin V-FITC (Invitrogen) and BD Horizon™ Fixable Viability Dye eFluor™ 780 (BD Biosciences) and acquired within 1-2 hours of staining.

Gating Strategy

Debris was excluded using FSC-A vs. SSC-A. Next, single cells were selected using FSC-A vs. FSC-H. Then, cells negative for Fixable Viability Dye were identified as viable cells. For thymocyte gating, viable single cells were then gated on CD4 vs. CD8. Thymocytes were gated as $CD4^+$, $CD8^+$, $CD4^+CD8^+$ (double positive, DP), or $CD4^-CD8^-$ (double negative, DN). DN cells were then gated on CD44 vs. CD25. DN cells were gated as $CD44^+CD25^-$ (DN1), $CD44^+CD25^+$

(DN2), $CD44^{-}CD25^{+}$ (DN3), and $CD44^{-}CD25^{-}$ (DN4). Cells from spleen and lymph nodes were similarly gated to remove debris then select for single viable cells. $CD5^{+}$ cells were selected and then gated on CD4 vs. CD8 to identify $CD4^{+}$ T cells ($CD4^{+}CD8^{-}$) and $CD8^{+}$ ($CD4^{-}CD8^{+}$). Further gating schemes can be found in CHAPTER 3:

Western Blot Analysis

Thymuses were processed into single-cell suspensions. Samples were then incubated and eluted from a nylon wool column to isolate thymocytes (95). Cells were resuspended in the appropriate amount of 2x Laemmli buffer and resolved on a 10% gel, then transferred to PVDF membrane. The following primary antibodies were used: FAM49B Rabbit PolyAb (Proteintech, 1:1000, 5% BSA-TBST) and β-tubulin Rabbit PolyAb (Proteintech, 1:1000, 5% BSA-TBST). Anti-rabbit IgG (Cell Signalling Technology, 1:5000, 5% milk-TBST) was used as the secondary antibody. Western blots were visualized with high contrast western blotting film (Diamed).

Statistical Analysis

Graphs were generated on GraphPad Prism 8. Statistical analyses were performed using GraphPad Prism 8. The statistical tests and *P*-values are specified in the figure legends. *P*-values < 0.05 were considered significant. Outliers were removed using the Grubb's-outlier test.

CHAPTER 3: RESULTS

3.1 Generation of *Fam49b* T cell conditional knockout

To study the role of FAM49B in lymphocytes, a T cell conditional knockout was generated. Mice with a *Fam49b* knockout-first allele (tm1a allele) on a C57BL/6J background were obtained from NorCOMM2. The tm1a allele has a promoter-driven cassette flanked by FRT sites inserted to disrupt *Fam49b*. The cross of a $Fam49b^{+/tm1a}$ mouse with a Flp recombinase mouse resulted in the removal of the Flp cassette, producing the tm1c allele (Figure 3.1 A). The tm1c allele is a functionally wild-type *Fam49b* allele, with exon 6 flanked by loxP sites. Mice were bred to homozygosity for $Fam49b^{tm1c}$ as well as for $Slc11a1^{G169}$ (Figure 3.1 C, top right mouse), a wild-type allele for *Salmonella* resistance. As *Slc11a1* is essential in restricting the growth of *Salmonella* (96), the *Slc11a1* mutant allele present on the C57BL/6 background of the conditional allele could obscure any phenotype associated with *Fam49b* alleles. Therefore, the wild-type allele, $Slc11a1^{G169}$, from the strain BcA17 was introduced through serial backcrosses to mice carrying the tm1c allele.

Simultaneously, $Fam49b^{tm1c/tm1c}$ mice were crossed with ubiquitous Meox-Cre recombinase mice. The tm1c allele in the presence of Cre recombinase yields the deletion of floxed exon 6 and produces the knockout tm1d allele (Figure 3.1 B). Mice homozygous for tm1d were non-viable; therefore, $Fam49b^{+/tm1d}$ were selected for further breeding. Mice with Cre recombinase under the control of *Lck*, a T cell-specific promoter, were crossed with $Fam49b^{+/tm1d}$ mice, generating B6.Tg(*Lck*-Cre)$Fam49b^{+/tm1d}$ mice (Figure 3.1 C, top left mouse).

The tm1c allele in the presence of Cre under the control of *Lck* would produce a T cell-specific deletion of *Fam49b*. Thus, a cross of B6.Tg(*Lck*-Cre)$Fam49b^{+/tm1d}$ mice with $Fam49b^{tm1c/tm1c}$ mice generated the necessary control (B6.Tg(*Lck*-Cre)$Fam49b^{tm1c/+}$) and experimental (B6.Tg(*Lck*-Cre)$Fam49b^{tm1c/tm1d}$) mice when carrying the transgene *Lck*-Cre (Figure

3.1 C). B6.Tg(*Lck*-Cre)*Fam49b*$^{tm1c/+}$ mice, also known as B6.Tg(*Lck*-Cre)*Fam49b*$^{flox/+}$, have one copy of wild-type *Fam49b* in T cells. B6.Tg(*Lck*-Cre)*Fam49b*$^{tm1c/tm1d}$ mice, also known as B6.Tg(*Lck*-Cre)*Fam49b*$^{flox/-}$, have no functional copies of *Fam49b* in T cells. Previous work has shown that mice with one copy of wild-type *Fam49b* were phenotypically equivalent to mice homozygous for wild-type *Fam49b*. All offspring carried one copy of *Slc11al*^{G169}.

The initial breeding scheme, although effective, was not optimal with only 50% of mice bred having the appropriate genotype. In a second breeding scheme, *Lck*-Cre mice were crossed with *Fam49b*^{tm1c}-*Slc11al*^{G169} mice to produce B6.Tg(*Lck*-Cre)*Fam49b*$^{tm1c/tm1c}$ mice (Figure 3.1 D, top left mouse). These B6.Tg(*Lck*-Cre)*Fam49b*$^{tm1c/tm1c}$ mice were then crossed with *Fam49b*^{tm1c}-*Slc11al*^{G169} mice (Figure 3.1 D, top right mouse), generating the control (*Fam49b*$^{tm1c/tm1c}$) and T cell-conditional knockout (B6.Tg(*Lck*-Cre)*Fam49b*$^{tm1c/tm1c}$) mice, all homozygous for *Slc11al*^{G169}. Control mice are homozygous for the tm1c allele and therefore are functionally wild-type (B6.*Fam49b*$^{+/+}$). Experimental mice are also homozygous for the tm1c allele, but in the presence of *Lck*-Cre, exon 6 is deleted from both alleles and produces T cell-specific conditional knockout mice (B6.Tg(*Lck*-Cre)*Fam49b*$^{flox/flox}$). In this breeding scheme, all mice are used and are homozygous for tm1c.

Phenotypically, wild-type from the initial breeding scheme (B6.Tg(*Lck*-Cre)*Fam49b*$^{flox/+}$) and wild-type from the second breeding scheme (B6.*Fam49b*$^{+/+}$) are equivalent. The presence or absence of *Lck*-Cre did not affect the different phenotypes tested (*Salmonella* susceptibility, cellularity of lymphoid organs, FACS analyses) of the wild-type mice. Similarly, the T cell-conditional knockout mice from both schemes, B6.Tg(*Lck*-Cre)*Fam49b*$^{flox/-}$ and B6.Tg(*Lck*-Cre)*Fam49b*$^{flox/flox}$, are indistinguishable. As such, experiments in further investigations used mice from both breeding schemes.

To confirm the efficacy of the Cre-lox system acting on both alleles of tm1c in the second breeding scheme, western blots were performed. Previous attempts to confirm the conditional knockout model were inconclusive as a residual expression of FAM49B was detected, most likely from other non-lymphocyte cells. As the thymus is largely composed of lymphocytes, the thymi were collected and processed. The single-cell suspensions were incubated with nylon wool to which more adherent cells, such as B cells, antigen-presenting cells (APCs), or epithelial cells attach. The eluted fraction with fewer adherent cells corresponds to a purified fraction of thymocytes. These purified thymocytes were then lysed and run on a western blot. In the presence of Cre, under the T cell-specific promoter *Lck*, FAM49B expression in the thymus is completely abrogated (Figure 3.1 E). This confirms the successful conditional knockout using the second breeding scheme (Figure 3.1 D).

3.2 Immunophenotyping of Fam49b T cell conditional knockout

3.2.1 Fam49b deletion in T cells results in reduced T cell number in the spleen without affecting T cell maturation in the thymus: In the T cell-conditional knockout model, hematology and immunophenotyping of the spleen and thymus were completed to look at the subsets of lymphoid and myeloid populations. Previous work showed that the original ENU full knockout mice, $Fam49b^{Ity15/Ity15}$, exhibited a significant decrease in the proportion of $CD8^+$ T cells in the spleen (93); however there were no abnormalities in blood counts or thymus composition. When comparing T cell-conditional knockout (B6.Tg(*Lck*-Cre)$Fam49b^{flox/-}$ or B6.Tg(*Lck*-Cre)$Fam49b^{fl/fl}$) with wild-type (B6.Tg(*Lck*-Cre)$Fam49b^{flox/+}$ or B6. $Fam49b^{+/+}$), there were no significant differences in hematologic parameters for both macrophage, monocyte, neutrophil, or lymphocyte populations (Table 2). In the spleen and thymus, there were no differences in total

cell numbers (Figure 3.2 A, C respectively). In the spleen, CD5, a T cell marker, was used to identify T cells and subsequently the identification of $CD4^+$ and $CD8^+$ T cells. There was a depletion of $CD5^+$ T cells (Figure 3.2 B, left) in the T cell-conditional knockout, which appears to mainly be driven by a decrease in $CD8^+$ T cells (Figure 3.2 B, right). This is similar to findings in the full knockout of *Fam49b*, but interestingly myeloid-specific conditional knockout models of *Fam49b* (B6.Tg(*Lysm*-Cre)*Fam49b*$^{fl/fl}$) did not show a decrease in T cells (93), pointing to an intrinsic role of *Fam49b* in T cells causing this T cell reduction.

To examine the source of this decrease in T cells, the development of the lymphocyte compartment was assessed in the thymus and compared between control (B6.*Fam49b*$^{+/+}$) and T cell-specific knockout (B6.Tg(*Lck*-Cre)*Fam49b*$^{fl/fl}$). When gating CD4 vs. CD8, there were no differences in the double-negative (DN, $CD8^-CD4^-$), double-positive (DP, $CD8^+CD4^+$) or single-positive (SP: $CD8^+$ and $CD4^+$) thymocytes (Figure 3.2 D). Further analysis of the DN thymocytes into DN1 to DN4 populations using CD25 vs. CD44 was completed, which did show genotypic differences. T cell-conditional knockout (B6.Tg(*Lck*-Cre)*Fam49b*$^{fl/fl}$) exhibited a decrease in DN4 (P-value = 0.048), which seems to be compensated for with an increase in DN1 (P-value = 0.004) (Figure 3.2 E). Although there are differences in the progression from DN1 to DN4 populations, there is no gross abnormality seen in the development of thymocytes as they move from DN to DP and into their determined fate as SP $CD4^+$ or $CD8^+$ T cells. As such, no gross developmental aberration was found to be responsible for the decrease in T cells in the periphery.

3.2.2 T cell deletion of Fam49b reduces the pool of naïve T cells: To further immunophenotype lymphocytes from the spleen, naïve and effector T cell phenotypes were identified using the expression of CD44 vs. CD62L cell surface markers (Figure 3.3 A). $CD44^{hi}$ is characteristic of

effector T cells while CD62L^{hi} is a marker for naïve or antigen-inexperienced T cells. CD44^{hi}CD62L^{hi} T cells are considered central memory (CM) T cells. T cell-conditional knockout (B6.Tg(*Lck*-Cre)*Fam49b*$^{fl/fl}$) splenocytes display a reduction in naïve CD4^{+} and CD8^{+} T cells (Figure 3.3 B). The absence of *Fam49b* in T cells caused a shift away from a naïve phenotype which does not impact the percentage of effector and CM T cells.

3.2.3 Impaired activation of Fam49b depleted T cells at steady state in vivo: Further evaluation of effector or memory T cell phenotypes were investigated through additional T cell activation markers: CD44, CD69, and CD25. As described previously, CD44 is a marker of effector T cells, while CD69 and CD25 are indicators of early T cell activation. Splenocytes were isolated from both genotypes and cultured for 5 hours with a combination of αCD3 and αCD28 or PMA and ionomycin, as well as an unstimulated condition. αCD3 and αCD28 activate T cells through interactions with costimulatory molecules, which is more comparable to physiological mechanisms. PMA/ionomycin is unspecific and causes a rapid influx of calcium leading to a large increase in T cell activation. T cell-conditional knockout (B6.Tg(*Lck*-Cre)*Fam49b*$^{fl/-}$ or B6.Tg(*Lck*-Cre)*Fam49b*$^{fl/fl}$) CD4^{+} T cells following stimulation with PMA/ionomycin displayed significantly heightened levels of activation, with an elevation of all three markers (Figure 3.4 A-C). In addition, increased % CD4^{+}CD69^{+} with CD3/CD28 stimulation was observed (Figure 3.4 C). T cell-conditional knockout CD8^{+} T cells demonstrated a more robust T cell activation phenotype with elevated % CD44^{hi} and % CD25^{+} with and without stimulation compared to control (B6.Tg(*Lck*-Cre)*Fam49b*$^{fl/+}$ or B6.*Fam49b*$^{+/+}$) (Figure 3.4 D, E). Of note, the T cell activation phenotype was more pronounced in CD8^{+} T cells compared to CD4^{+} T cells, in line

with the stronger T cell depletion phenotype seen in $CD8^+$ T cells. Overall, the depletion of *Fam49b* in T cells demonstrated higher levels of T cell activation.

3.2.4 FACS analysis of T helper cytokines in Fam49b T cell-specific conditional knockout: In addition to activation, cytokine production was assessed to determine if there was a T cell polarization for either Th1 (IFN-γ, TNF-α), Th2 (IL-5, IL-13), or Th17 (IL-17α) phenotype. There was a predominant production of Th1 cytokines after stimulation in both groups. In *Fam49b* deficiency (B6.Tg(*Lck*-Cre)$Fam49b^{fl/-}$ or B6.Tg(*Lck*-Cre)$Fam49b^{fl/fl}$), $CD8^+$ T cells produced higher levels of Th1 cytokine IFN-γ, following 5-hour stimulation with CD3/CD28 as well as with PMA/ionomycin (Figure 3.5 A). Moreover, $CD8^+$ T cells from conditional knockout mice produced marginally higher levels of Th2 cytokine IL-13 (Figure 3.5 D). Otherwise, there were no significant differences in intracellular levels of TNF-α (Figure 3.5 B), IL-17α (Figure 3.5 C), or IL-5 (Figure 3.5 E). CD4+ T cells consistently did not show significantly different responses in cytokine production (Figure 3.5 A-E). Analogous to the patterns seen for activation, there was a more distinct effect in $CD8^+$ T cell cytokine production with no detectable differences in $CD4^+$ T cell cytokine production.

3.3 *Fam49b* T cell-specific conditional knockout during challenge with *Salmonella* infection

3.3.1 Fam49b deficiency in T cell confers mild Salmonella susceptibility: To observe if this T cell activation phenotype affects clinical outcomes to infection, the T cell-conditional knockout mice were challenged with *Salmonella*. As previously described, *Fam49b* was discovered in an ENU mutagenesis screen for susceptibility to *Salmonella,* as the full knockout mouse model ($Fam49b^{Ity15/Ity15}$) was significantly more susceptible than the wild-type ($Fam49b^{+/+}$). The

myeloid-specific conditional knockout (*Lysm*-Cre) mice also succumbed to the infection faster than control mice (93), given the importance of the myeloid lineage in host defence against *Salmonella*. T cells are crucial in the clearance of *Salmonella* as T cell-conditional knockout mice succumb to infection (97). As such, the lymphoid-specific conditional knockout was also challenged with *S.* Typhimurium infection. The deletion of *Fam49b* in T cells resulted in a decrease in survival when compared to the control (Figure 3.6 A), which is a much milder susceptibility phenotype in comparison to full knock out and myeloid conditional knockout models (93). There were no differences in the spleen index at day 5 post-infection (Figure 3.6 B) and CFUs showed only a marginal increase in bacterial load in the liver (Figure 3.6 C). Although there is this mild susceptibility phenotype, the deletion of *Fam49b* in T cells does not seem to greatly affect the outcomes of acute *Salmonella* infection.

3.3.2 Salmonella infection does not alter T cell numbers and activation in the spleen of T cell-specific conditional Fam49b knockout: Immunophenotyping during infection was performed. Mice were infected with 1000 CFUs of *S.* Typhimurium and on day 5 post-infection, splenocytes were isolated, stained, and analyzed. As seen in uninfected mice, *Salmonella*-infected T cell-conditional (B6.Tg(*Lck*-Cre)*Fam49b*$^{fl/-}$ or B6.Tg(*Lck*-Cre)*Fam49b*$^{fl/fl}$) mice exhibited a lower $CD5^+$ T cells count compared to infected wild-type (B6.Tg(*Lck*-Cre)*Fam49b*$^{fl/+}$ or B6.*Fam49b*$^{+/+}$) mice, which was due to the diminished percentage of $CD8^+$ T cells (Figure 3.7 A). We did not observe a difference in the activation phenotype of $CD4^+$ and $CD8^+$ T cells between wild-type and conditional knockout mice (Figure 3.7 C and 7D). During infection there is an increase in % $CD44^{hi}$ $CD8^+$ T cells (Figure 3.7 C) only in wild-type mice. This was not

observed in the T cell-conditional knockout which may be explained by the fact that activation levels were already high at steady-state and they did not increase during *Salmonella* infection.

3.3.3 FACS analysis of T helper cytokines in Fam49b T cell-specific conditional knockout during Salmonella infection: We measured T cell cytokine production by FACS to assess possible differences between wild-type and conditional knockout mice in T cell polarization during *Salmonella* infection. The splenocytes were left untreated or stimulated with CD3/CD28 or PMA/ionomycin for 5 hours. The cells were then fixed and permeabilized for intracellular staining. Comparable to what was seen in steady-state lymphocytes, we observed a predominant Th1 bias. In wild-type mice we observe an increase in the percentage of IFN-γ producing $CD8^+$ T cells during infection (22.30% ± 0.22 at day 5 versus 15.77% ± 0.94 at day 0) upon stimulation with PMA/ionomycin (Figure 3.8 A compared to Figure 3.5 A). In the T cell-conditional knockout, we did not observe an increase in IFN-γ producing $CD8^+$ T cells following infection as the percentage was already elevated at day 0 and did not induce a stronger response (27.07% ± 1.05 at day 5 versus 27.48% ± 1.03 at day 0) (Figure 3.8 A and Figure 3.5 A). Although there was no increase in the percentage of IFN-γ producing $CD8^+$ T cells in conditional knockout mice, the levels were significantly higher than those observed in wild-type mice after PMA/ionomycin (Figure 3.8 A). A higher percentage of IL-13 producing $CD8^+$ T cells (Figure 3.8 D) during infection was observed in the T cell-conditional knockout compared to wild-type control after stimulation with CD3/CD28 as previously observed at day 0. No major differences in $CD4^+$ T cell cytokine production were observed between the two groups (Figure 3.8 A-E). In the conditional knockout mice, the profile of cytokine expression during infection reflects observed differences in cytokine production seen at steady state. Overall, in response to a

challenge with *Salmonella* infection, B6.Tg(*Lck*-Cre)*Fam49b*$^{fl/fl}$ mice did not induce a stronger CD8$^+$ T cell activation or cytokine response than seen at steady-state.

3.4 Cell death and proliferation in T cell-specific conditional knockout of *Fam49b*

3.4.1 Fam49b deficiency does not affect T cell death: The T cell depletion phenotype, seen at both steady-state and during *Salmonella* infection, was further investigated. Cell death was evaluated as a possible source in the reduction of T cell numbers. Phosphatidylserine (PS) is a phospholipid found on the inner leaflet of the cellular membrane. During apoptosis, caspase activity disrupts the organization of the lipid bilayer and PS can be found on the outer surface of cells (98). PS is a signal for phagocytes to rapidly clear the apoptotic cells. Annexin V binds to negatively charged phospholipids such as PS and when used in conjunction with a membrane-impermeable vital dye, can be used to estimate the level of apoptosis (99) (Figure 3.9 A). Vital dye (Fixable Viability Dye) is actively expelled from live cells and therefore only labels necrotic or dying cells. Therefore, live cells are negative for both Annexin V and viability dye. Early apoptotic cells have externalized PS and stain Annexin V$^+$ but continue to be negative for the viability dye. Late apoptotic cells have accumulated the membrane-impermeable vital dye and are double positive for Annexin V and Fixable Viability Dye. Lastly, necrotic cells lose the structural integrity of the lipid bilayer and Annexin V no longer binds and is then single positive for the viability dye. The T cell-conditional knockout (B6.Tg(*Lck*-Cre)*Fam49b*$^{fl/fl}$) had mildly elevated early apoptotic CD4$^+$ T cells with a mean of 16.28% ± 0.49 in comparison to the 11.79% ± 1.11 seen in control (B6.*Fam49b*$^{+/+}$) (Figure 3.9 B). No differences in apoptosis were seen for T cells overall (CD5$^+$) as well as CD8$^+$ T cells. Although *Fam49b* deletion in T cells was associated with a minor increase in CD4$^+$ T cell death, it does not account for the depletion

seen in T cells overall ($CD5^+$) or $CD8^+$ T cells. This rules out the likelihood that cell death is responsible for the decrease in $CD8^+$ T cells observed in conditional knockout mice.

3.4.2 Fam49b deficiency in T cells exhibits elevated proliferative ability: As there were no major developmental issues or cell death, we then evaluated T cell proliferation as a mechanism for T cell reduction. Splenocytes were stained with CFSE and cultured for 5 days with αCD3 and αCD28. Fluorescent CSFE links to intracellular molecules and is retained in the cell. With each subsequent division, fluorescence decreases incrementally, and cell division can be traced. The proliferation index was calculated as the total number of cell divisions divided by the number of dividing cells. The proliferation index takes into consideration cells that have undergone at least one division and therefore only account for responsive cells, providing a more informative indicator. T cell-conditional knockout (B6.Tg(*Lck*-Cre)*Fam49b*$^{fl/fl}$) lymphocytes demonstrated a greater proliferative activity, with an elevated proliferation index compared to control (B6.*Fam49b*$^{+/+}$) for both $CD4^+$ T cells (Figure 3.10 A) and $CD8^+$ T cells (Figure 3.10 B). Reduced number of T cells found in the spleen does not seem to be due to impaired cell proliferation. However, there is a possibility that the increased proliferation rate is a homeostatic response to T cell depletion.

3.5 The role of naïve T cells in *Fam49b* T cell-specific conditional knockout

3.5.1 Fam49b-deficient naïve T cells display an elevated activation phenotype: Homeostatic proliferation results in the conversion of T cells from naïve to a memory phenotype (100). If the elevated proliferation rate in T cells observed is due to a homeostatic response, it may also be responsible for the elevated T cell activation and cytokine production seen. Given the need to

parse the differences between an intrinsic elevated activation and a secondary effect of homeostatic proliferation, naïve T cell activity was evaluated. Spleen and lymph nodes (inguinal, axillary, brachial, cervical) were collected and cells were isolated. The cells were purified for the naïve T cell fraction (>92% purity, $CD44^{lo}CD62L^{hi}$) and incubated with CD3/CD28 or PMA/ionomycin for 18 hours to induce T cell activation *in vitro*. This effort was done to determine if there is an increased conversion of naïve T cells into effector T cells in the T cell-conditional knockout, B6.Tg(*Lck*-Cre)*Fam49b*$^{fl/fl}$. By focusing on naïve T cells, it eliminates T cells which may have been activated due to homeostatic expansion, providing a clearer picture.

After 18 hours, T cell proportions were found to have lower $CD8^+$ T cells in B6.Tg(*Lck*-Cre)*Fam49b*$^{fl/fl}$ when compared to B6.*Fam49b*$^{+/+}$ (Figure 3.11 A). This follows similar patterns seen in prior experiments with whole splenocytes (Figure 3.2 B) as well as under challenge with *Salmonella* (Figure 3.7 A). Following stimulation, naïve T cells ($CD44^{lo}CD62L^{hi}$) shifted to effector T cell phenotypes ($CD44^{hi}CD62L^{lo}$). The activation of naïve T cells seen in *Fam49b* deficiency was to a much greater extent than wild-type control, with effector T cells making up to 17.38% ± 4.49 of $CD4^+$ and 8.83% ± 2.15 of $CD8^+$ T cells in the conditional knockout in comparison to 2.55% ± 0.99 of $CD4^+$ and 1.65% ± 0.76 of $CD8^+$ T cells in wild-type (Figure 3.11 B). When looking at CD44 specifically, there was a significantly higher percentage of $CD44^{hi}$ in both $CD4^+$ (Figure 3.11 C, D) and $CD8^+$ (Figure 3.11 F, G) T cells in T cell-conditional knockout cells. CD69, an early activation marker, is transiently expressed upon activation and showed lower levels of expression in T cell-conditional knockout compared to wild-type controls (Figure 3.11 H). Altogether, these results may suggest that there is an intrinsic activation phenotype as higher levels of activation were observed in conditional knockout in all conditions including unstimulated.

3.5.2 Co-transfer of Fam49b knockout and wild type T cells transferred to lymphopenic hosts:
To examine whether *Fam49b* mutation perturbs normal differentiation of naïve T cells, we co-transferred purified naïve T cells from wild type and B6.Tg(*Lck*-Cre)*Fam49b*$^{fl/fl}$ mice into a lymphopenic host (*Tcrb*$^{-/-}$). In the T cell-conditional knockout (B6.Tg(*Lck*-Cre)*Fam49b*$^{fl/fl}$), the reduction of T cells in the periphery blurs any conclusion made as the activation phenotype may be secondary to homeostatic proliferation. In a host lacking T cells, transferred T cells undergo lymphopenia induced proliferation (LIP). By transferring wild-type and conditional knockout lymphocytes into the same lymphopenic host (*Tcrb*$^{-/-}$), both groups will be under identical environmental pressures and undergo lymphopenia induced proliferation. Naïve T cells were enriched from both wild-type control (C57BL/6), which were CD45.1^{+}, and B6.Tg(*Lck*-Cre)*Fam49b*$^{fl/fl}$, which were CD45.2^{+}. The cells were stained with CFSE and then mixed at a 1:1 ratio. 6x10^{6} cells were injected in *Tcrb*$^{-/-}$ mice and spleen and lymph nodes were collected after 7 days (Figure 3.12 A).

Before injection, cells were analyzed to confirm if the proportions of CD45.1^{+} : CD45.2^{+} was 1:1, which was found to be 52:45 (Figure 3.12 B) with a naïve T cell purity (CD44^{lo}CD62L^{hi}) of 96%. After 7 days, spleen (Figure 3.12 C) and lymph node (Figure 3.12 E) were analyzed for populations of CD45.1^{+} from wild-type and CD45.2^{+} from T cell-conditional knockout. Wild-type CD45.1^{+} T cells were found to have reached and populated the secondary lymphoid organs. On the other hand, the T cell-conditional knockout CD45.2^{+} were only found at very small proportions in both spleen (Figure 3.12 C) and lymph node (Figure 3.12 E). 23.08% ± 0.69 of the wild-type CD45.1^{+} T cells in the spleen and 48.00% ± 2.35 of CD45.1^{+} T cells in the lymph node retained their naïve phenotype; however, the CD45.2^{+} T cells were almost all converted to effector or

memory-type T cells with only 0.48% ± 0.13 of T cells in the spleen and 2.74% ± 0.52 of T cells in the lymph node retaining a naïve phenotype (Figure 3.12 E and F respectively).

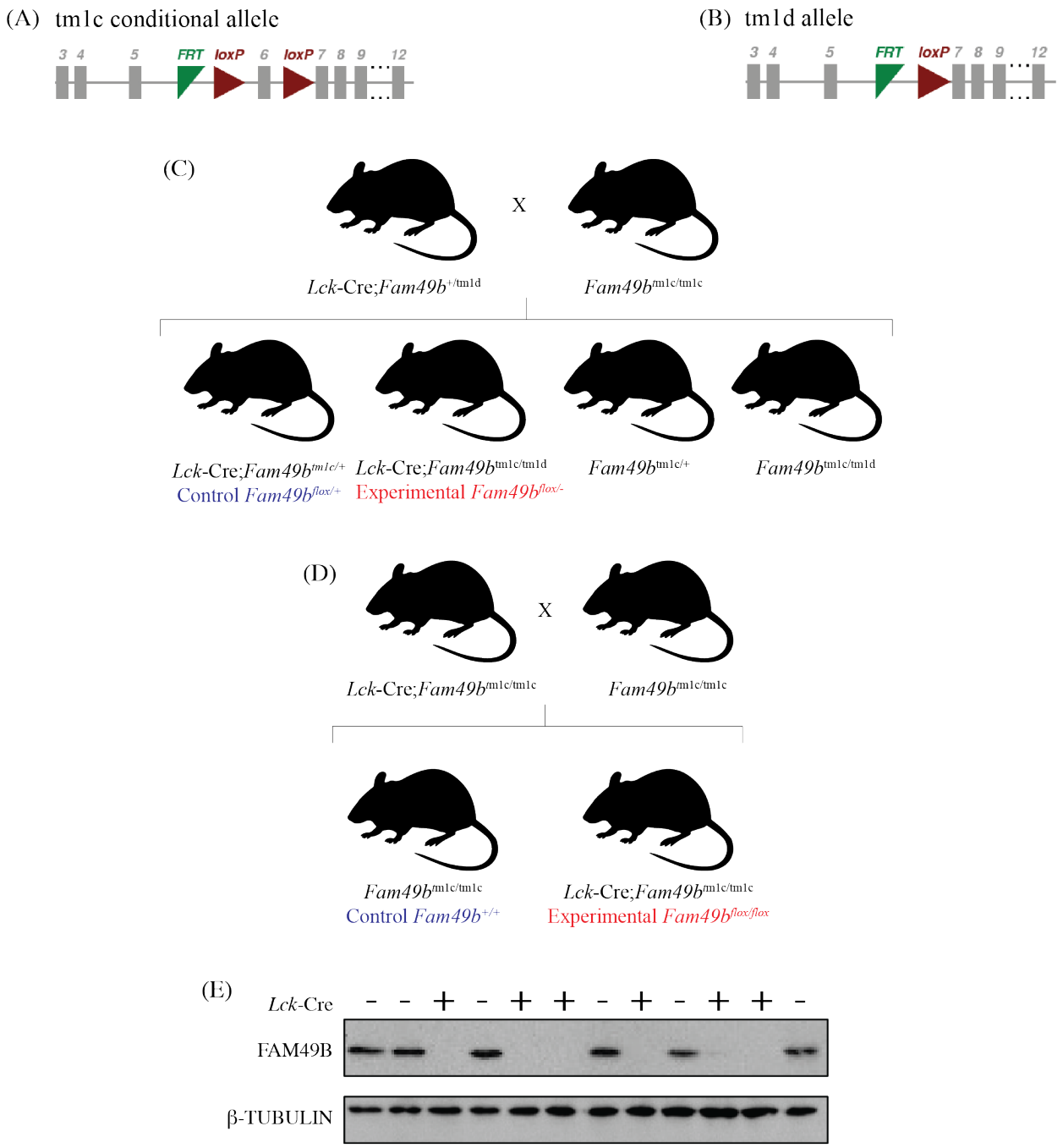

Figure 3.1: Generation of T cell conditional knockout of *Fam49b*. (A) The tm1c allele is a functionally wild-type allele with loxP sites that would be recombined in the presence of Cre recombinase. (B) The tm1d allele is the knockout allele. (C) The cross between heterozygous mice (*Fam49b*$^{+/tm1d}$) carrying the transgene Cre under the control of T cell promoter (*Lck*-Cre) and mice

homozygous for tm1c produces control and experimental mice when carrying the transgene. (D) The cross of two homozygous tm1c mice, with one carrying the transgene *Lck*-Cre. (E) Western blotting of FAM49B and β-TUBULIN in thymocytes in control and experimental mice from (D), confirming successful conditional knockout.

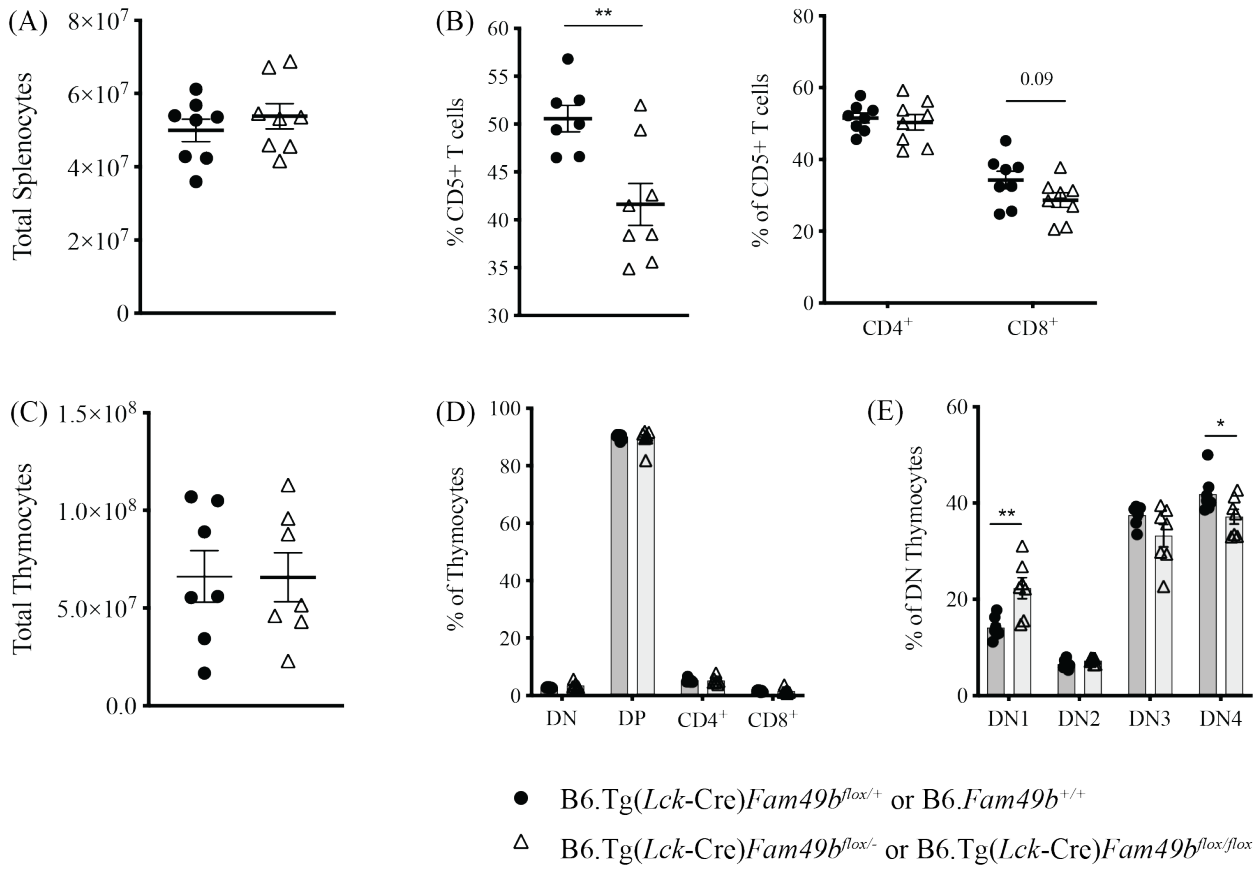

Figure 3.2: FAM49B deletion in T cells results in reduced T cell numbers in the spleen without affecting T cell maturation in the thymus. Flow cytometry analysis of wild-type (B6.Tg(*Lck*-Cre*)Fam49b*$^{flox/+}$ or B6.*Fam49b*$^{+/+}$) and conditional knockout (B6.Tg(*Lck*-Cre*)Fam49b*$^{flox/-}$ or B6.Tg(*Lck*-Cre)*Fam49b*$^{flox/flox}$) naïve mouse spleens (A-B) and thymus (C-E) is shown. (A) Total splenocyte numbers for wild type and conditional knockout mice. (B) Percentage of $CD5^+$, $CD4^+$ and $CD8^+$ lymphocytes. (C) Total thymocyte numbers for wild-type and conditional knockout mice. (D and E) Percentage of thymocytes by developmental stages. Thymocytes develop through double-negative stages (stages 1 to 4) to double-positive stages before maturating to either $CD4^+$ or $CD8^+$ single positive. The results shown indicate the mean±SEM for data pooled from two independent experiments (n=8 for spleen and n=7 for thymus per genotype). Multiple t-tests using the Holm-Sidak method were used to assess significance.

* P<0.05; ** P<0.01.

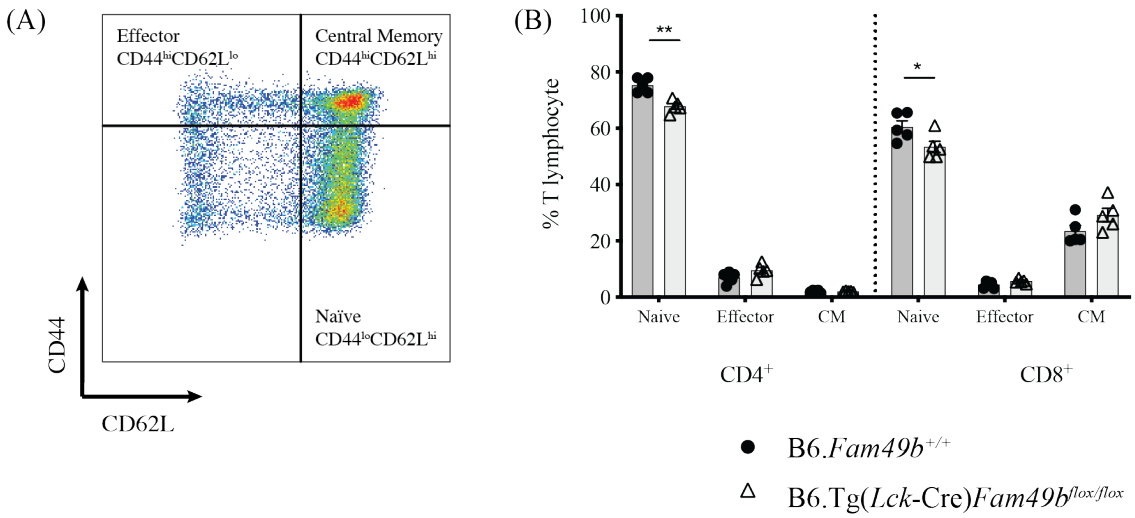

Figure 3.3: T cell deletion of *Fam49b* reduces the pool of naïve T cells. (A) CD44 and CD62L were used to gate lymphocytes from the spleen of B6.*Fam49b*$^{+/+}$ and B6.Tg(*Lck*-Cre)*Fam49b*$^{flox/flox}$ mice. T cells lose CD62L following activation while CD44 is a marker for effector T cells. Cells double positive for CD44 and CD62L are CM T cells, naive T cells are CD44^{lo}CD62L^{hi} and effector T cells are CD44^{hi}CD62L^{lo}. (B) Percentage of naïve, effector and memory CD4^{+} and CD8^{+} T cells recovered from the spleen. The results shown indicate the mean±SEM for data from one experiment (n=5 per genotype). Data representative of two independent experiments. Multiple t-tests using the Holm-Sidak method were used to assess significance. * P<0.05; ** P<0.01.

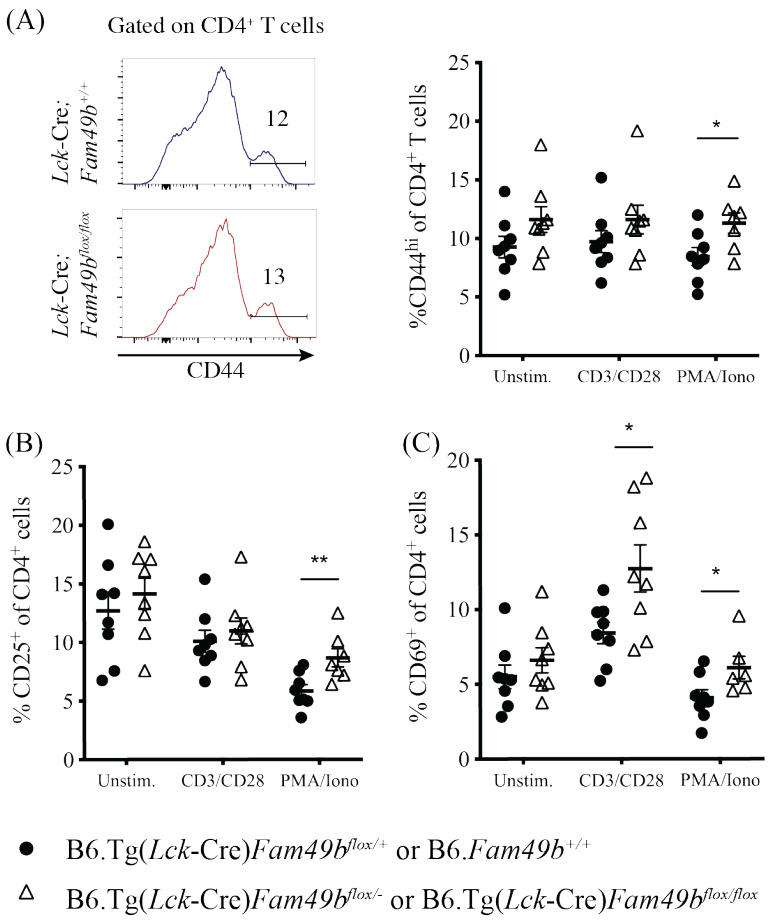

Figure 3.4: Impaired activation of FAM49B depleted T cells at steady state *in vivo*.

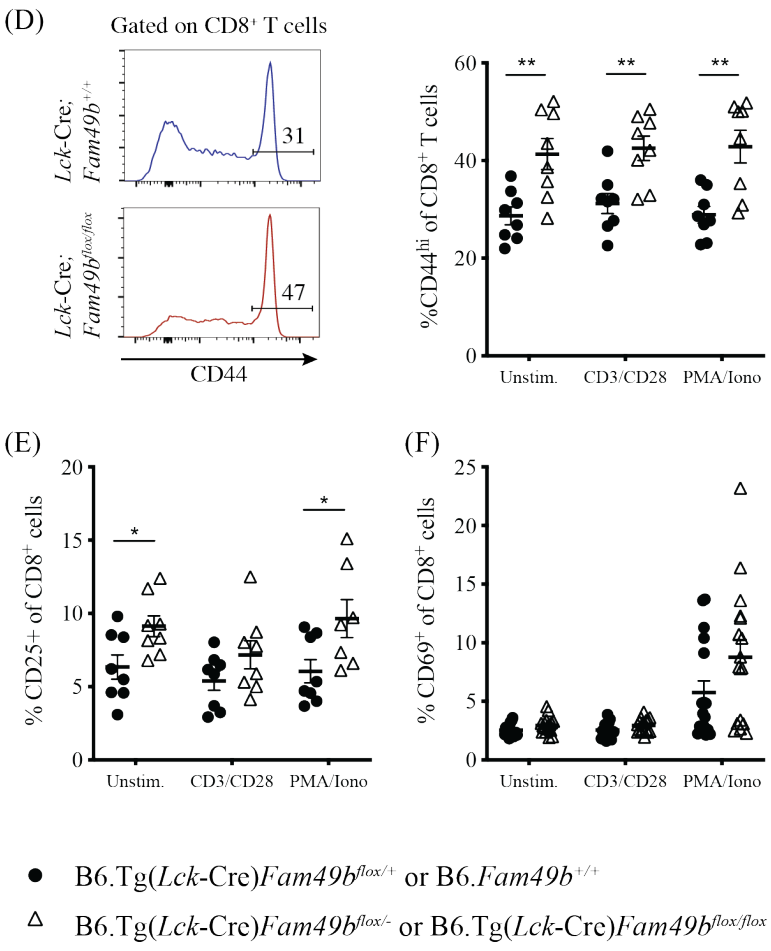

Figure 3.4: Impaired activation of FAM49B depleted T cells at steady state *in vivo*. Splenocytes were isolated from wild-type (B6.Tg(*Lck*-Cre)*Fam49b*$^{flox/+}$ or B6.*Fam49b*$^{+/+}$) and conditional knockout (B6.Tg(*Lck*-Cre)*Fam49b*$^{flox/-}$ or B6.Tg(*Lck*-Cre)*Fam49b*$^{flox/flox}$) mice and cultured with CD3/CD28 or PMA/Ionomycin for 5 hours. (A) Representative histograms for CD44 expression gated on CD4$^+$ T cells in unstimulated samples (left panels). Percentage of (A) CD44 (right panel), (B) CD25, and (C) CD69 of resting (unstim), CD3/CD28, or PMA/Ionomycin stimulated CD4$^+$ T cells. Representative histograms for CD44 expression gated on CD8$^+$ T cells in unstimulated samples (D, left panels). Percentage of CD44 (D, right panel), CD25 (E), and CD69 (F) of resting (unstim), CD3/CD28, or PMA/Ionomycin stimulated CD8$^+$ T cells. The results shown in the right panels indicate the mean±SEM for data pooled from two independent

experiments (n=8 per genotype). Data representative of four independent experiments. Multiple t-tests using the Holm-Sidak method were used to assess significance. * $P<0.05$; ** $P<0.01$.

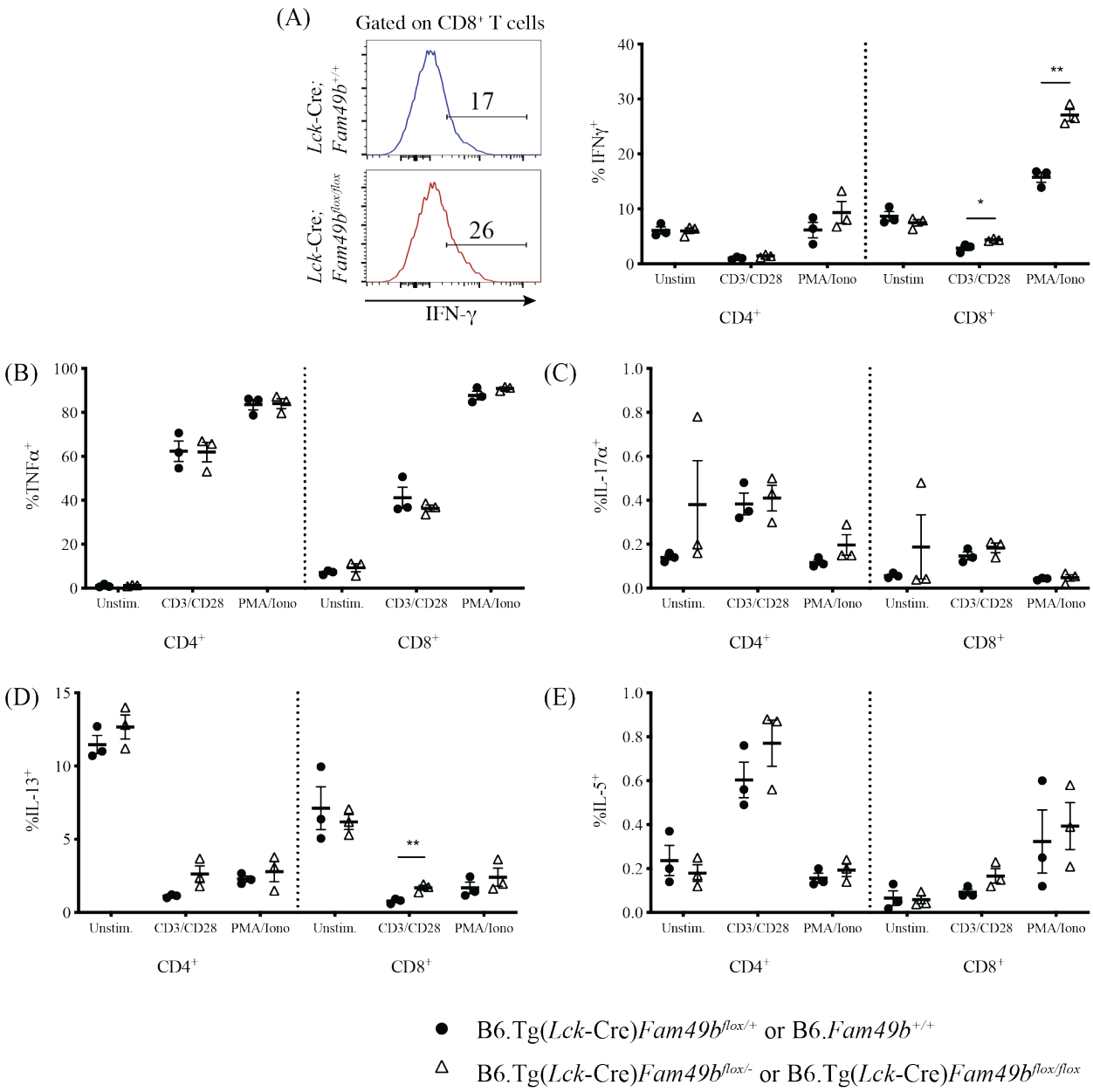

Figure 3.5: FACS analysis of T helper cytokines in *Fam49b* T cell-specific conditional knockout. Splenocytes were isolated from wild-type (B6.Tg(*Lck*-Cre)*Fam49b*$^{flox/+}$ or B6.*Fam49b*$^{+/+}$) and conditional knockout (B6.Tg(*Lck*-Cre)*Fam49b*$^{flox/-}$ or B6.Tg(*Lck*-Cre)*Fam49b*$^{flox/flox}$) mice and treated with CD3/CD28 or PMA/Ionomycin for 5 hours. Percentages of gated, specific cytokine-producing T helper cells per spleen were determined by intracellular cytokine staining for Th1 (IFN-γ and TNF-α), Th2 (IL-5 and IL-13), and Th17 (IL-17α) cytokines.

Representative histograms for $CD8^+$ IFN-γ expression following activation of T cells with PMA/ionomycin (A, left panels). Percentage of $CD4^+$ and $CD8^+$ IFN-γ (A, right panel); TNF-α (B); IL-17α (C); IL-13 (D); and IL-5 (E). The results shown indicate the mean±SEM for data from one experiment (n=3 per genotype). Data representative of four independent experiments. Multiple t-tests using the Holm-Sidak method were used to assess significance. * $P<0.05$; ** $P<0.01$.

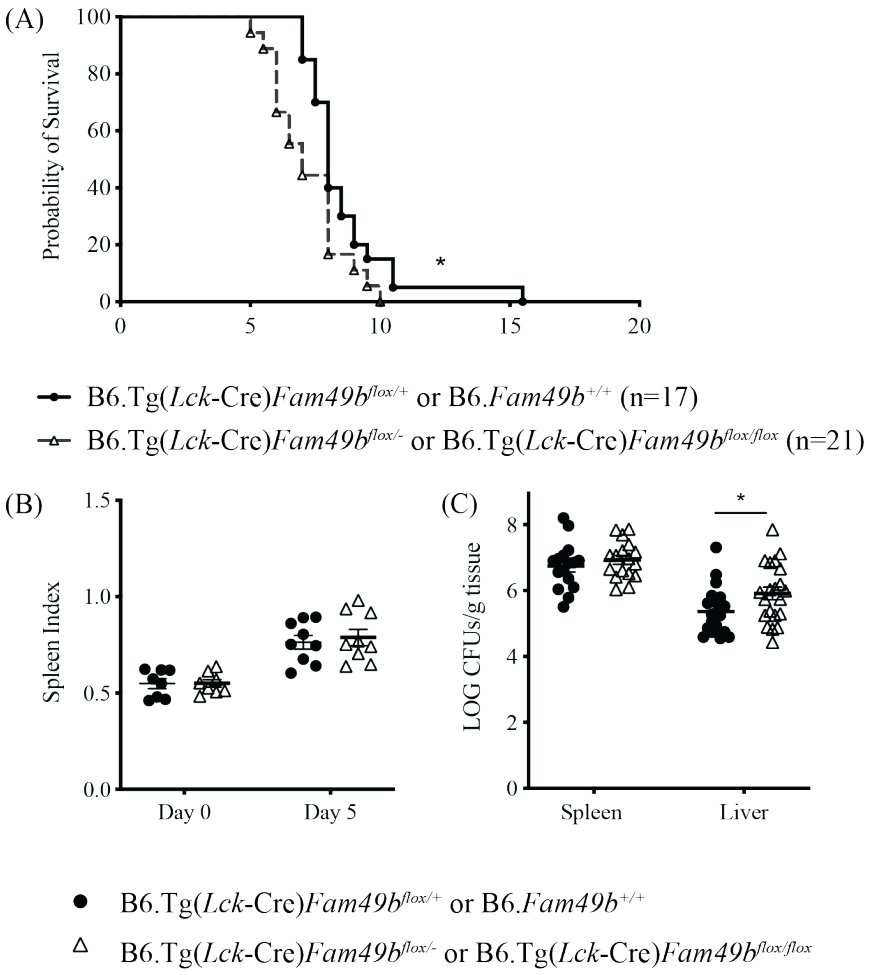

Figure 3.6: *Fam49b* deficiency in T cell confers mild *Salmonella* susceptibility. (A) Survival curves of wild-type (B6.Tg(*Lck*-Cre*)Fam49b*$^{flox/+}$ or B6.*Fam49b*$^{+/+}$) and conditional knockout (B6.Tg(*Lck*-Cre*)Fam49b*$^{flox/-}$ or B6.Tg(*Lck*-Cre)*Fam49b*$^{flox/flox}$) mice infected with *S.* Typhimurium. Data was pooled from three independent experiments. Logrank (Mantel-Cox test) was used to assess significance. *P<0.05. (B) Spleen index prior to and after infection in wild-type and conditional knockout mice. The results shown indicate the mean±SEM for data pooled from two independent experiments (n=9 per genotype). (C) Bacterial load in spleen and liver collected day 5 post-*S.* Typhimurium infection. The results shown indicate the mean±SEM for data pooled from four independent experiments. For (B) and (C) multiple t-tests using the Holm-Sidak method were used to assess significance. * P<0.05.

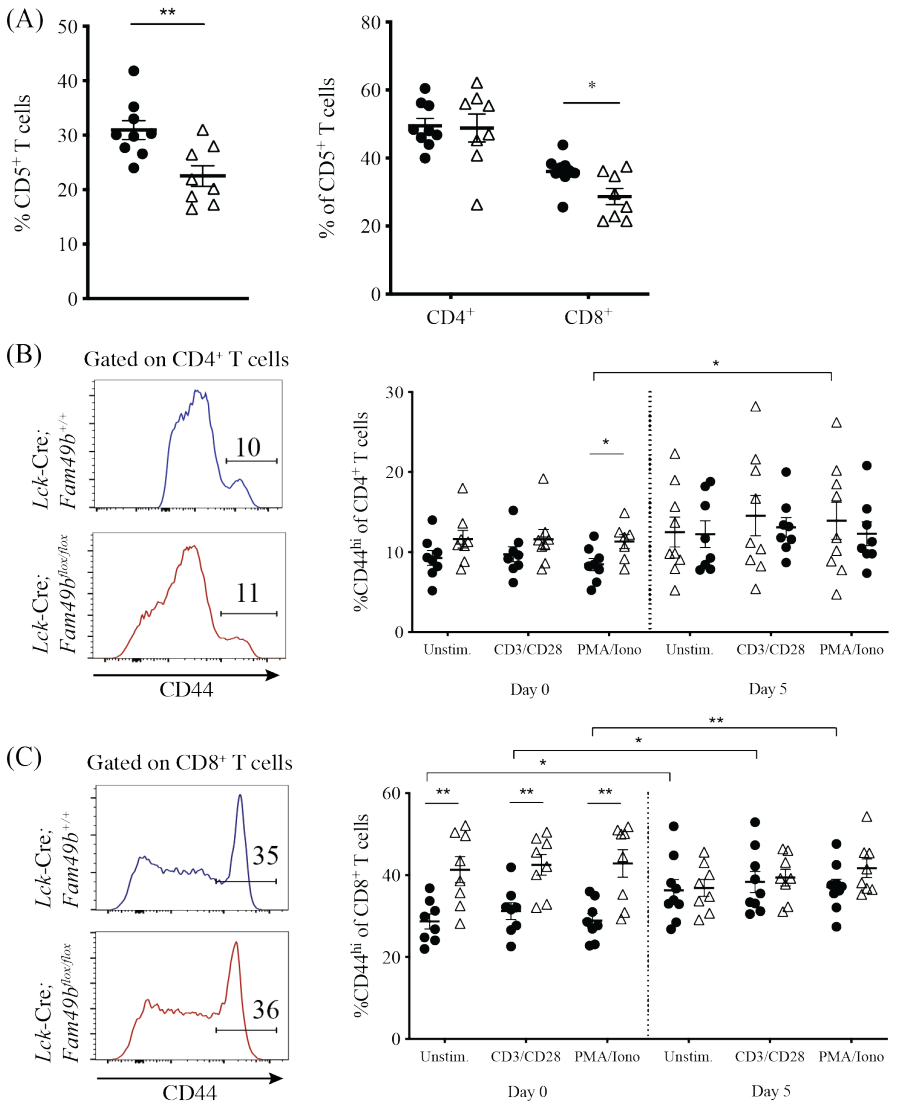

Figure 3.7: *Salmonella* infection does not alter T cell numbers and activation in the spleen of T cell-specific conditional *Fam49b* knockout. Wild-type (B6.Tg(*Lck*-Cre)*Fam49b*$^{flox/+}$ or B6.*Fam49b*$^{+/+}$) and conditional knockout (B6.Tg(*Lck*-Cre)*Fam49b*$^{flox/-}$ or B6.Tg(*Lck*-Cre)*Fam49b*$^{flox/flox}$) mice were infected with *S.* Typhimurium and the spleens were collected on day 5 post-infection. Splenocytes were treated with CD3/CD28 or PMA/Ionomycin for 5 hours. (A) Percentage of CD5$^+$, CD4$^+$, and CD8$^+$ T lymphocytes during infection. Representative

histograms for CD44 expression of unstimulated $CD4^+$ (B, left) or $CD8^+$ (C, left). Percentage of CD44 of unstimulated (unstim), CD3/CD28 or PMA/Ionomycin stimulated $CD4^+$ (B, right) or $CD8^+$ (C, right) T cells during infection. The results shown indicate the mean±SEM for data pooled from two of four independent experiments (n=8 per genotype). Multiple t-tests using the Holm-Sidak method were used to assess significance. * $P<0.05$; ** $P<0.01$.

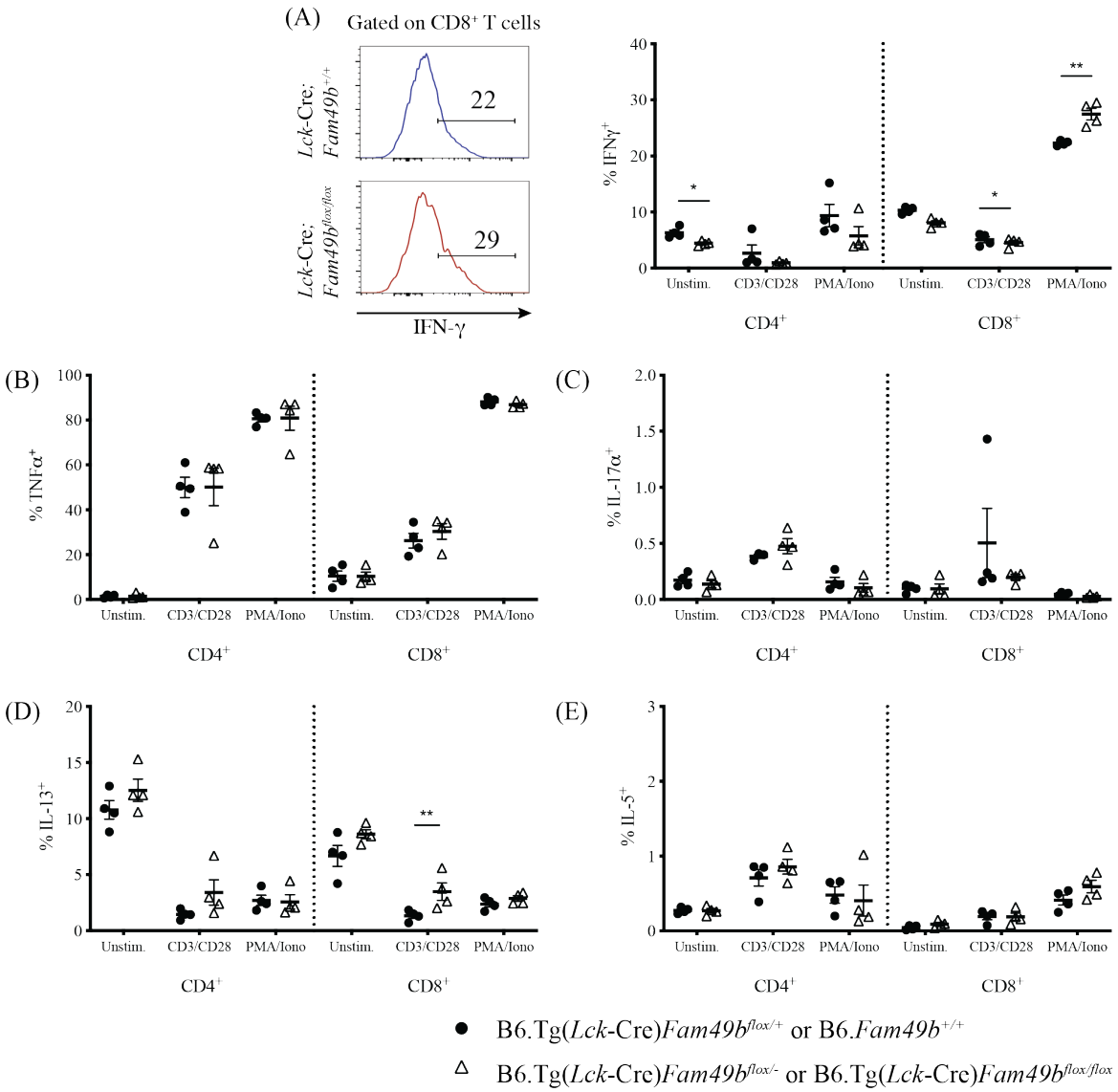

Figure 3.8: FACS analysis of T helper cytokines in *Fam49b* T cell-specific conditional knockout during *Salmonella* infection. Wild-type (B6.Tg(*Lck*-Cre)*Fam49b*$^{flox/+}$ or B6.*Fam49b*$^{+/+}$) and conditional knockout (B6.Tg(*Lck*-Cre)*Fam49b*$^{flox/-}$ or B6.Tg(*Lck*-Cre)*Fam49b*$^{flox/flox}$) mice were infected with *S.* Typhimurium and spleens were collected on day 5 post-infection. Splenocytes were treated with CD3/CD28 or PMA/Ionomycin for 5 hours. Percentages of gated, specific cytokine-producing T helper cells per spleen were determined by intracellular cytokine staining for Th1 (IFN-γ and TNF-α), Th2 (IL-5 and IL-13) and Th17 (IL-17α) cytokines. Representative histograms for CD8$^+$ IFN-γ expression following activation of T

cells with PMA/ionomycin (A, left panels). Percentage of $CD4^+$ and $CD8^+$ (A, right) IFN-γ; (B) TNF-α; (C) IL-17α ; (D) IL-13 and (E) IL-5 The results shown indicate the mean±SEM for data from one of three independent experiments (n=4 per genotype). Multiple t-tests using the Holm-Sidak method were used to assess significance. * $P<0.05$; ** $P<0.01$.

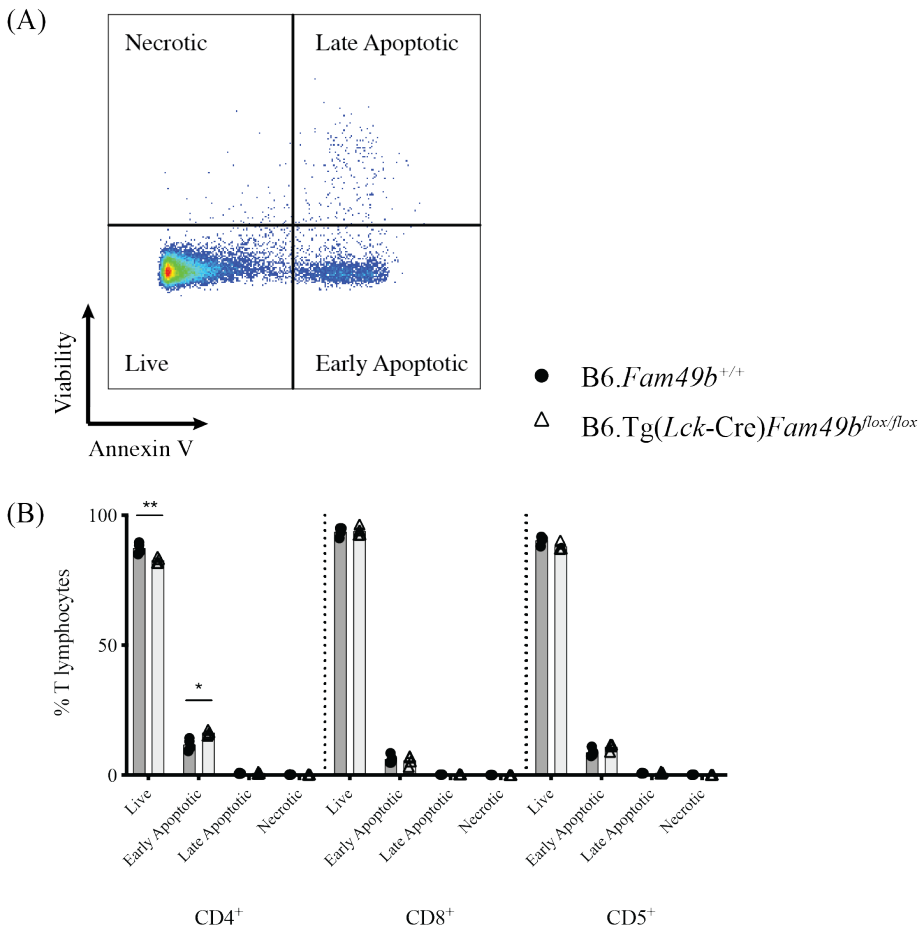

Figure 3.9: *Fam49b* deficiency does not affect T cell death. To assess cell death, splenocytes from B6.*Fam49b*$^{+/+}$ and B6.Tg(*Lck*-Cre)*Fam49b*$^{flox/flox}$ were stained with Fixable Viability Dye as well as Annexin V. (A) The gating strategy to assess apoptosis uses Annexin V, which stains PS, a marker of cell death. When gated against an impermeable viability dye, apoptosis can be evaluated. (B) Although not a grossly large difference, there is an increase in early apoptotic and a decrease in live cells in the B6.Tg(*Lck*-Cre)*Fam49b*$^{flox/flox}$ CD4^{+} T cells. However, this is not seen in CD5^{+} and CD8^{+} T cells. The results shown indicate the mean±SEM for data from one experiment (n=4 per genotype). Data is representative of two independent experiments. Multiple t-tests using the Holm-Sidak method were used to assess significance.

* P<0.05; ** P<0.01.

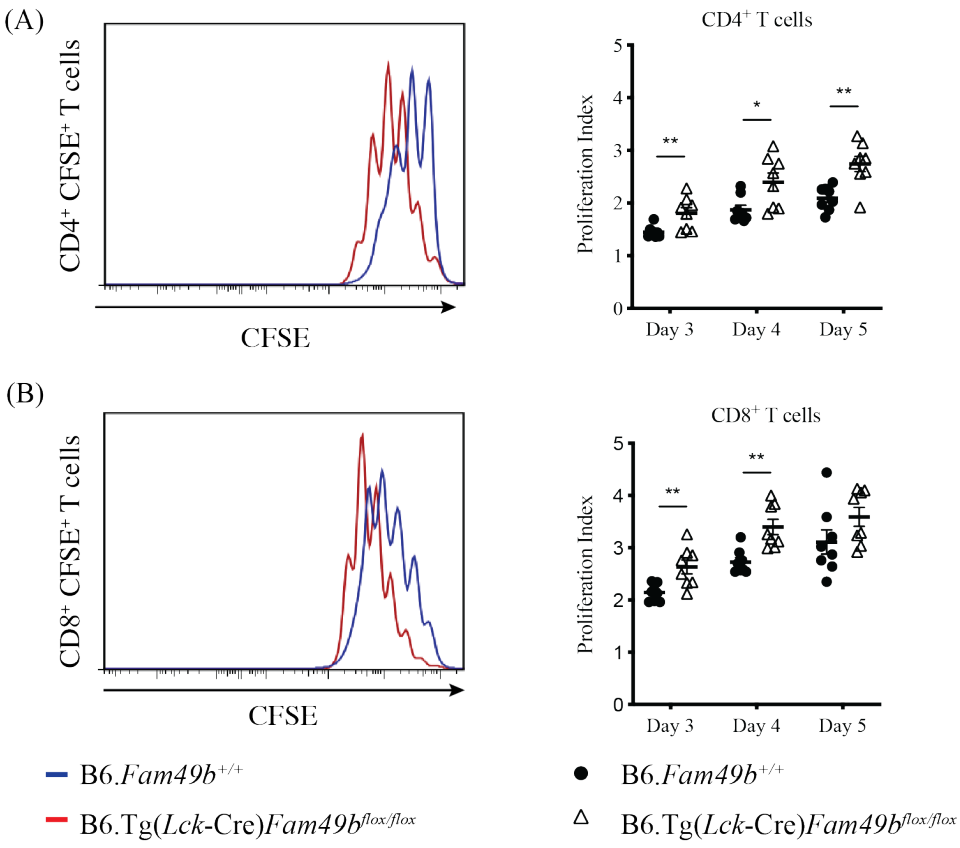

Figure 3.10: *Fam49b* deficiency in T cells exhibits elevated proliferative ability. Splenocytes were isolated from B6.*Fam49b*$^{+/+}$ and B6.Tg(*Lck*-Cre)*Fam49b*$^{flox/flox}$ and treated with .Carboxyfluorescein succinimidyl ester. To assess proliferation, CFSE stained splenocytes were cultured for 5 days with CD3/CD28 stimulus. On day 2, IL-2 was added to the cell culture media. Flow cytometry was used to analyze CFSE-labeled cells. Both CD4$^+$ (A) and CD8$^+$ (B) T cells lacking *Fam49b* proliferate at higher rates than wild-type T cells. Histograms of CFSE staining in CD4$^+$ and CD8$^+$ cells are shown on the left from representative samples. The results shown in the right panels indicate the mean±SEM for data pooled from two independent experiments (n=8 per genotype). Multiple t-tests using the Holm-Sidak method were used to assess significance. * P<0.05; ** P<0.01

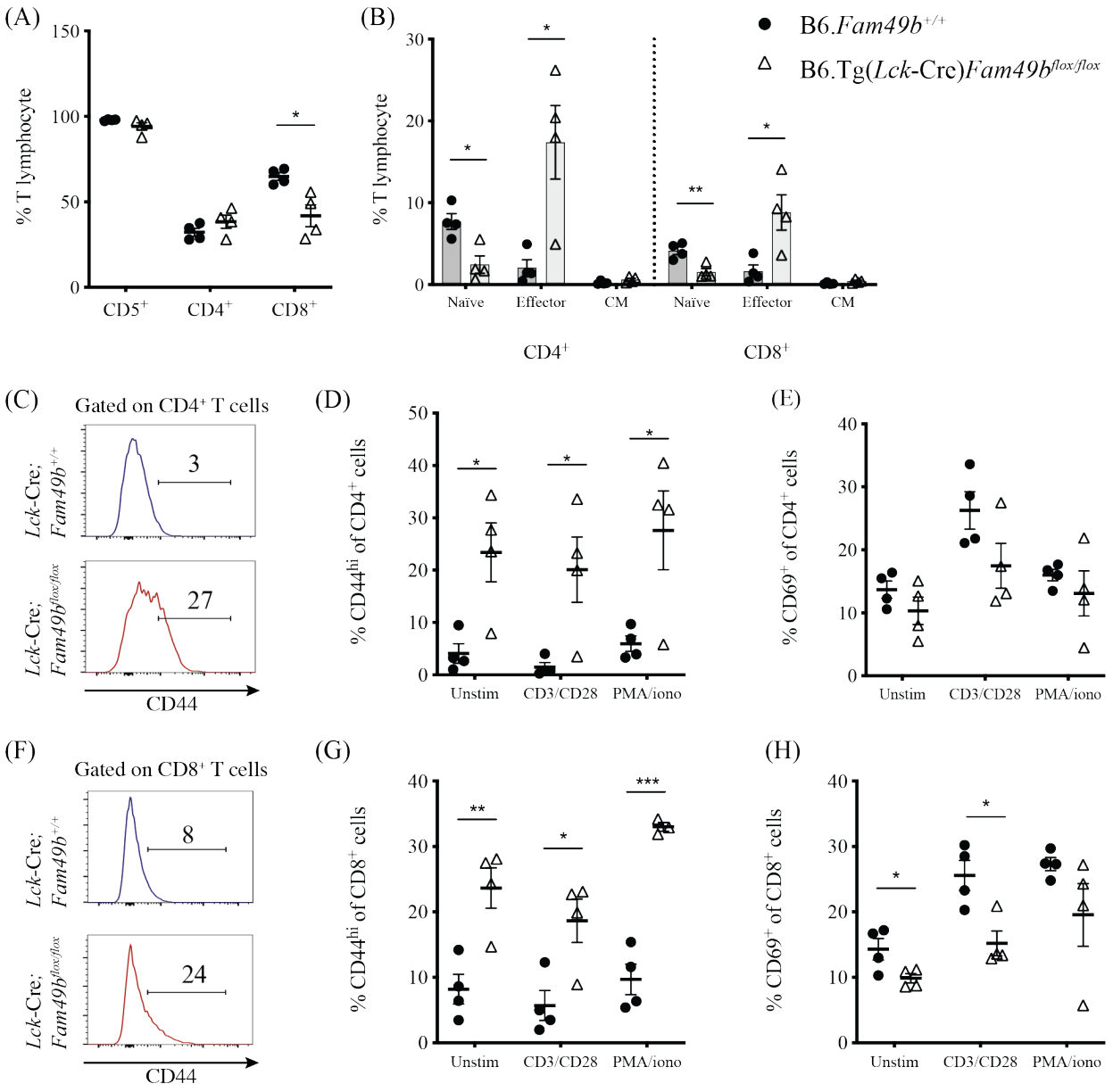

Figure 3.11: *Fam49b*-deficient naïve T cells display an elevated activation phenotype. Cells were isolated from the spleen and lymph nodes of B6.*Fam49*$^{+/+}$ and B6.Tg(*Lck*-Cre)*Fam49b*$^{flox/flox}$ mice and enriched for naive T cells (>92% purity). Naïve T cells were activated with CD3/CD28 and incubated for 18 hours. The activation of naïve T cells *in vitro* was assessed. (A) Percentage of CD5^{+}, CD4^{+}, and CD8^{+} T lymphocytes. (B) Percentage of naïve, effector, and CM T cells within the CD4^{+} and CD8^{+} populations. Representative histogram of CD44 expression gated on CD4^{+} (C)

or $CD8^+$ (F) naïve T cells. Percentage of $CD44^{hi}$ (D and G) and CD69 (E and H) expression on $CD4^+$ (D and E) and $CD8^+$ (G and H) naïve T cells. The results shown indicate the mean±SEM for data from one experiment (n=4 per genotype). Data is representative of two independent experiments. Multiple t-tests using the Holm-Sidak method were used to assess significance. * $P<0.05$; ** $P<0.01$; ***$P<0.001$.

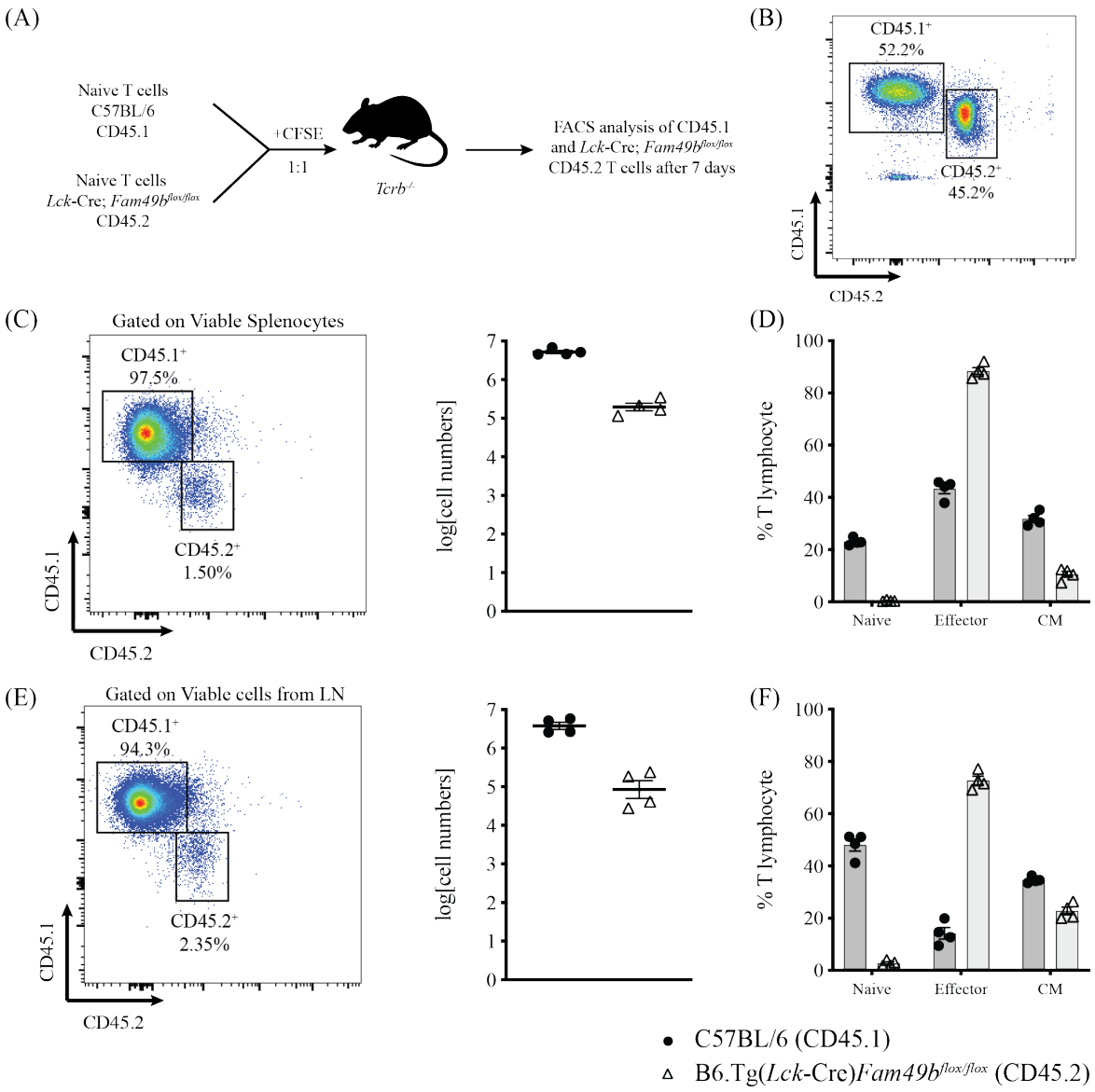

Figure 3.12: Co-transfer of *Fam49b* knockout and wild type T cells transferred to lymphopenic hosts. The spleen and lymph nodes were isolated from C57BL/6 (CD45.1) and B6.Tg(*Lck*-Cre)*Fam49b*$^{fl/fl}$ (CD45.2) mice and enriched for naive T cells (purity >95%). (A) Naive T cells were stained with CFSE and mixed at a 1:1 ratio. 6x10^6 cells were injected into *Tcrb*$^{-/-}$ mice. After 7 days, the spleen and lymph nodes were collected and analyzed by fluorescence-activated cell sorter (FACS). (B) Prior adoptive transfer, 1:1 mixed of CD45.1$^+$ and CD45.2$^+$ cells were analyzed through FACS to determine the ratio. (C, D) Representative gating for CD45.1 vs.

CD45.2 expression on spleen (C, left) and lymph nodes (D, left). Gating on CD45.1 vs. CD45.2 determined the number of T cells in the spleen (C, right) and lymph nodes (D, right). Percentage naïve, effector, and CM cells of conditional knockout and wild-type were determined through gating CD44 vs. CD62L in the spleen (D) and lymph node (F). The results shown indicate the mean±SEM for data from one experiment (n=4 per genotype).

Table 1: Genotyping Information

Marker	Sequences
Fam49b WT	Fam49b_wt_F: TAAGGCAATCCAGCATCCAGCCGATGAG Fam49b_wt_R: TTCCTTGTCTGGTAGCTCTGGCATCC
Intron 6-7	Fam49b_wt_F: TAAGGCAATCCAGCATCCAGCCGATGAG Fam49b Intron6-7-Rev: GACTTGCCCCATATTGCAATATGGAAG
Lck	15729: TGT GAA CTT GGT GCT TGA GG oIMR7338: CTA GGC CAC AGA ATT GAA AGA TCT oIMR7339: GTA GGT GGA AAT TCT AGC ATC ATC C oIMR8990: CAG GTT CTT GCG AAC CTC AT

Table 2: Hematology of B6.*Fam49b*$^{+/+}$ and B6.Tg.(Lck-Cre)*Fam49b*$^{flox/flox}$ mice.

Parameter	B6.*Fam49b*$^{+/+}$	B6.Tg.(Lck-Cre)*Fam49b*$^{flox/flox}$	P-value
WBCs x 10^9/L	6.525 ± 0.5188	6.338 ± 0.9034	0.8604
RBCs x 10^{12}/L	10.16 ± 0.2299	10.54 ± 0.1394	0.1767
Hemoglobin g/L	150.6 ± 2.405	156.0 ± 1.722	0.0929
Hematocrit L/L	0.4865 ± 0.009430	0.4990 ± 0.005379	0.2688
MCV fL	48.00 ± 0.2673	47.25 ± 0.2500	0.0596
MCH pg	14.85 ± 0.2163	14.79 ± 0.2167	0.8412
MCHC g/L	309.8 ± 3.544	312.6 ± 3.134	0.5531
Platelets x 10^9/L	1012 ± 54.84	977.0 ± 47.07	0.6381
Neutrophils %	14.38 ± 3.540	11.00 ± 1.035	0.3757
Lymphocytes %	76.88 ± 4.442	83.25 ± 0.7500	0.1789
Monocytes %	7.625 ± 1.322	4.500 ± 0.6268	0.0508
Neutrophils x 10^9/L	0.9938 ± 0.2760	0.7113 ± 0.1523	0.3853
Lymphocytes x 10^9/L	4.946 ± 0.3927	5.271 ± 0.7455	0.7055
Monocytes x 10^9/L	0.4975 ± 0.1121	0.2800 ± 0.04833	0.0965

Complete blood cell counts B6.*Fam49b*$^{+/+}$ and B6.Tg.(Lck-Cre)*Fam49b*$^{fl/fl}$. Data was pooled from two independent experiments. Data are presented as mean±SEM, and n represents the number of mice. Results are considered significant when comparing B6.*Fam49b*$^{+/+}$ and B6.Tg.(Lck-Cre)*Fam49b*$^{fl/fl}$ (two-tailed Student's t-test).

CHAPTER 4: DISCUSSION

4.1 Role of *Fam49b* in T cells

In previous studies, *Fam49b* has been identified as a RAC1-mediator of actin polymerization, which is involved in multiple cellular processes. In particular, our group's recent work has shown *Fam49b* to be involved in phagocytosis and neutrophil migration. It seems this cytoskeletal effect on immune cells induces a susceptibility phenotype in the myeloid-specific conditional knockout of *Fam49b* (93). Cytoskeleton-dependent processes such as antigen presentation, polarization, and signalling are important in a variety of immune cell types and may affect their function.

In this project, the experiments up to date have illustrated the role of *Fam49b* in T cells at steady-state and during *Salmonella* infection. Loss of *Fam49b* in T cells seems to affect T cell numbers, specifically with a depletion in $CD8^+$ T cells in secondary lymphoid organs. Given the role of *Fam49b* in cell migration, the possibility that cell mobility within the thymus was affecting lymphocyte maturation was considered. Double negative development or β-selection entails T cell receptor (TCR) rearrangement; cells that have not successfully produced a functional pre-TCR will undergo cell death at the DN3 stage. If the cells have gone through β-selection, they become double positive $CD4^+CD8^+$ thymocytes with a fully assembled T cell receptor. The cells then undergo positive and negative selection to transition into single positive thymocytes. During the maturation of thymocytes in the context of *Fam49b* deficiency, there were differences seen in the DN1 and DN4 development stages. Although these mild changes during DN development were seen, it did not grossly affect development into single positive thymocytes.

We then looked at cell death as a possible mechanism for lymphocyte depletion and observed a mild apoptotic phenotype in $CD4^+$ T cells, but no differences in $CD8^+$ T cell death. This indicates that cell death in secondary lymphoid organs is likely not the process causing low

$CD8^+$ T cell numbers. Consistent with this finding, PDAC cells with *Fam49b* silencing were not associated with apoptosis, with no changes in cytochrome c release or caspase 9 or 3 activation (88). More investigation into the source of the lymphocyte depletion must continue to determine the source of this abnormality.

4.2 T cell activation and actin polymerization

During T cell activation, several mechanisms require cytoskeleton rearrangement to efficiently recognize and respond to antigen. Processes such as synapse formation, cellular adhesion, cell polarization, receptor sequestration, and downstream signalling are dependent on proper actin modulation (101).

T cell activation and cytokine production were evaluated through FACS analysis to further study the role of *Fam49b.* In both $CD4^+$ and $CD8^+$ T cells, an elevated T cell activation phenotype was seen, most strongly in $CD8^+$ T cells. Associated with increased activation was elevated cytokine production of both IFN-γ and IL-13. This is in line with previously published work, in which a genome-wide CRISPR knockout screen identified *Fam49b* as a T cell activation regulator (90).

Besides RAC1, previous studies in our labs identified other possible interactors of FAM49B through a BioID assay (Yuki KE, Sladek R and Malo D, unpublished). One of these candidates, AHNAK, is a scaffold protein with multiple functions, including cytoskeletal regulation (102). AHNAK has also been identified as a regulator of T cell calcium signalling and TCR activation (103). FAM49B may interact with these essential T cell activation modulators, which then affects the activation states of T cells.

Interestingly, this activation phenotype was also seen in the unstimulated groups for $CD8^+$ T cells. This shows that without *in vitro* T cell activation, the $CD8^+$ T cells were activated at steady-

state. In the *Fam49b* conditional knockout, T cells may be hyperactivated at baseline due to their direct involvement in T cell activation. Another possibility is the T cell depletion may have induced a homeostatic response for proliferation, which is associated with a memory T cell state. Both possibilities must be investigated further.

4.3 Lymphopenia induced proliferation (LIP)

Typically, the anti-apoptotic signal of IL-7 in conjunction with TCR interaction with self-peptide MHC will support the survival of naïve T cells. During lymphopenia, high concentrations of IL-7 and other γ-chain cytokines such as IL-2 and IL-15 cause naïve T cells to undergo homeostatic proliferation with subsequent conversion into a memory T cell phenotype (100,104). Many of these memory-like T cells are reactive to self-peptide and subsequently LIP has been associated with auto-immunity (105).

The T cell-specific conditional knockout of *Fam49b* showed enhanced T cell proliferation of both $CD4^+$ and $CD8^+$ T cells. Lymphopenia induced proliferation involves several mechanisms in response to acute T cell depletion (104). Given homeostatic proliferation results in the conversion of T cells from naïve to a memory phenotype (100), it may be responsible for elevated proliferation with associated activated T cell states. Hematology (Table 2) does not suggest that B6.Tg(*Lck*-Cre)*Fam49b*$^{fl/fl}$ are lymphopenic, with no significant differences in lymphocyte populations in the blood. Nevertheless, the reduced T cells in the peripheral lymphoid organs may still generate a homeostatic proliferative response. Of note, $CD8^+$ lymphocytes have been found to be more sensitive to homeostatic proliferation than $CD4^+$ T cells (106), and in this model the phenotype has been much more heavily seen in the $CD8^+$ compartment. But the dilemma remains, whether there is true T cell activation versus homeostatic proliferation induced memory-phenotype T cells.

An initial experiment was done to determine the activation capability of naïve T cells *in vitro*. Following enrichment for naïve T cells and stimulation or rest for 18 hours, there was an enhanced expression of T cell activation markers in the conditional knockout. However, these results are not conclusive as to whether there is an activation phenotype, as the unstimulated control also displayed this difference in T cell activation. It seems that in the T cell-conditional knockout, the naïve cells do not need any stimulus as they are already intrinsically activated at steady-state. In addition, when assessing purity there was a significant difference in naïve T cells between genotypes after enrichment with the T cell-conditional knockout at a mean of 93% compared to the wild-type purity of 97% (P-value of 0.0139). The lower purity in the T cell-conditional knockout may account for some of the elevated activation seen.

Further studies need to be done to delineate the two possibilities, which would require controlling the environment and removing the confounding factors. To parse this difference, an adoptive co-transfer was completed to determine if there is an intrinsic proliferative ability in cells lacking *Fam49b.* Wild-type and conditional knockout cells were transferred 1:1 into lymphopenic *Tcrb*$^{-/-}$ mice. Unfortunately, only recipient wild-type cells were recovered which is suggestive of possible rejection of the knockout *Fam49b* T cells. However, all mice used were on a C57BL/6 background and rejection is less likely. Another possibility may be related to the mobility of the conditional knockout T cells. This may affect their survival due to their inability to home to the appropriate niche within the spleen and lymph nodes. This experiment will need to be repeated with adjustments to the experimental design.

4.4 *Salmonella* Infection model of *Fam49b* T cell-conditional knockout

During infection with *S.* Typhimurium of the *Fam49b* T cell-conditional knockout model, there was a minimal difference in survival and bacterial load seen. Also, immunophenotyping

during infection found little changes in T cell activation and cytokine production. It appears the wild-type mice were pushed to a higher activation level following infection, while the conditional knockout has enhanced activation prior to infection and was not able to be elevated any further.

Previously the full knockout, *Fam49b*$^{Ity15/Ity15}$, was also challenged with *Plasmodium berghei* (cerebral malaria) and coxsackie virus B3 and did not show differential survival (unpublished data). Although no clinical phenotype was seen with these infections as well as with *Salmonella* in the T cell-conditional knockout, there is a possibility that a more T-cell dependent infection may show a phenotype. Many of the previously tested infections are acute, with mice succumbing within 7 days. Given the adaptive response typically takes 5-7 days to mount, a more chronic infection may elucidate the role of *Fam49b* in the T cell response.

4.5 Implications

Overall, the work displayed in my thesis investigates *Fam49b* as a potential T cell activation modulator. The role of *Fam49b* as a cytoskeletal regulator affects a variety of cell types within the context of both cancer tumorigenesis and the immune cells. In PDAC, they pointed to FAM49B expression as a possible therapeutic target as the downregulation of FAM49B expression led to greater metastatic potential (88). In T cells, investigators hypothesized the possibility of *Fam49b* as an immunotherapy target as deficiency led to greater T cell activation (90). Given this conflicting hypothetical application of *Fam49b*, more work needs to be done to investigate the role of *Fam49b* broadly. In particular, it is important to now conclusively determine if *Fam49b* is a regulator of T cell activation.

CHAPTER 5: CONCLUSIONS & FUTURE DIRECTIONS

5.1 Conclusions

Despite advancements in access to clean water and hygiene in the developing world, food-borne pathogens remain a large health burden. The study of host defence responses to infectious diseases is important to better understand the disease state and also provides other potential promising applications.

Fam49b was identified through an ENU mutagenesis screen as a novel gene causing susceptibility to *Salmonella*. Further study of the gene in cell-specific conditional knockout models can delineate the role of the gene within different cell types. In the T cell-specific conditional knockout, *Fam49b* was found to induce only a mild *Salmonella* susceptibility phenotype. Immunophenotyping through FACS analysis elucidated the potential role of *Fam49b* as a regulator of T cell activation. Further study into its role is needed to conclusively identify *Fam49b* as a modulator of lymphocyte activation and the possible implication during immune challenge.

5.2 Future Directions

The most pertinent experiment to complete (which was not possible due to the COVID-19 pandemic) at this time is to repeat the adoptive co-transfer experiments at a 1:1 ratio for wild-type and conditional knockout naïve T cells into a lymphopenic host. The initial attempt to do this was inconclusive due to the low levels of *Fam49b*-depleted T cells recovered after one week T cells transfer. The first step is now to reattempt this experiment and harvest the spleens 1 day post injection. This would provide insight as to if the conditional knockout naïve T cells reach the secondary lymphoid organs at all or if they are being rejected after they have reached their niche. An alternative approach could be to co-transfer these cells into an irradiated mouse with a similar background as the T cell-conditional knockout mice. If the cells do successfully graft, we can

determine if there is an intrinsic enhancement of T cell activation and proliferation in the absence of *Fam49b.*

To understand the cause of the T cell depletion, many other assays can be completed. IL-7, IL-2, and IL-15 serum levels can be assessed to determine if there are differences in anti-apoptotic cues. An addition to current flow cytometry panels could be to add IL-7R to see if there is a possible difference in response to survival cues. Similarly, culturing the T cells with IL-7 or IL-15 stimulus can indicate if the cells respond differently to the γ-chain cytokines.

Besides survival, the ability of cells to home properly to secondary lymphoid organs can be investigated for a potential cause in lymphocyte reduction. Using sphingosine 1 phosphate receptor (S1PR) antagonists, such as FTY720, will block the egress of lymphocytes and cause an accumulation within lymphoid tissues. Differences in this accumulation can point to a defect in T cell homing. In addition, exploring the potential mobility defects of *Fam49b* deletion in T cells can be done through *in vitro* assays similar to those done for neutrophils in previous studies (93). Preliminary experiments done by Jérémy Postat (laboratory of Dr. Judith Mandl) showed that there were changes in the mobility of T cells *in vitro* associated with *Fam49b* deletion, and further studies may help to elucidate the role of *Fam49b* cytoskeletal modulation on lymphocyte migration and subsequent effects on the immune responses.

Although infection with *S.* Typhimurium showed a substantial susceptibility phenotype in the full and myeloid-specific knockout mice, this was not seen in the T cell-conditional knockout. Mice succumb to acute *S.* Typhimurium infection within approximately 7 days; however, a more chronic T cell-dependent infection will allow for enough time for the adaptive response to mount and possibly see a stronger clinical phenotype. In an attempt to induce an adaptive immune response, the T cell-specific conditional knockout mice were challenged with attenuated

Salmonella strains. These strains were missing important virulence genes and induce a slower infectious process; however, no altered response was seen with the less virulent bacteria. To further investigate the implications of *Fam49b* in T cells, challenge with a pathogen with a T cell-dependent immune response may observe a greater altered response. For example, a well-described model of chronic lymphocytic choriomeningitis virus (LCMV) infection has been used to investigate T cell function, in particular CTL activity (107). As the *Fam49B* T cell-conditional knockout model has shown a predominantly $CD8^+$ T cell phenotype, infection with a chronic strain of LCMV may illustrate the impacts of the gene in T cells.

Overall, these studies will provide a greater depth of understanding in the host defence response and have possible wider implications as *Fam49b* likely plays a significant role in many cell types.

REFERENCES

1. Kirk MD, Pires SM, Black RE, Caipo M, Crump JA, Devleesschauwer B, et al. World Health Organization Estimates of the Global and Regional Disease Burden of 22 Foodborne Bacterial, Protozoal, and Viral Diseases, 2010: A Data Synthesis. PLOS Med [Internet]. 2015 Dec 3;12(12):e1001921. Available from: https://doi.org/10.1371/journal.pmed.1001921
2. Kariuki S, Revathi G, Kariuki N, Kiiru J, Mwituria J, Hart CA. Characterisation of community acquired non-typhoidal Salmonella from bacteraemia and diarrhoeal infections in children admitted to hospital in Nairobi, Kenya. BMC Microbiol [Internet]. 2006;6(1):101. Available from: https://doi.org/10.1186/1471-2180-6-101
3. Brenner FW, Villar RG, Angulo FJ, Tauxe R, Swaminathan B. Salmonella Nomenclature. J Clin Microbiol [Internet]. 2000;38(7):2465–7. Available from: https://jcm.asm.org/content/38/7/2465
4. Spanò S. Mechanisms of Salmonella Typhi Host Restriction BT - Biophysics of Infection. In: Leake MC, editor. Cham: Springer International Publishing; 2016. p. 283–94. Available from: https://doi.org/10.1007/978-3-319-32189-9_17
5. Buckle GC, Walker CLF, Black RE. Typhoid fever and paratyphoid fever: Systematic review to estimate global morbidity and mortality for 2010. J Glob Health [Internet]. 2012 Jun;2(1):10401. Available from: http://www.ncbi.nlm.nih.gov/pmc/articles/PMC3484760/
6. Crump JA, Luby SP, Mintz ED. The global burden of typhoid fever. Bull World Health Organ [Internet]. 2004 May;82(5):346–53. Available from: http://www.ncbi.nlm.nih.gov/pmc/articles/PMC2622843/
7. Imanishi M, Newton AE, Vieira AR, Gonzalez-Aviles G, Kendall Scott ME, Manikonda

K, et al. Typhoid fever acquired in the United States, 1999-2010: epidemiology, microbiology, and use of a space-time scan statistic for outbreak detection. Epidemiol Infect. 2015 Aug;143(11):2343–54.

8. Lynch MF, Blanton EM, Bulens S, Polyak C, Vojdani J, Stevenson J, et al. Typhoid fever in the United States, 1999-2006. JAMA. 2009 Aug;302(8):859–65.

9. Parry CM, Hien TT, Dougan G, White NJ, Farrar JJ. Typhoid Fever. N Engl J Med [Internet]. 2002 Nov 28;347(22):1770–82. Available from: https://doi.org/10.1056/NEJMra020201

10. Chanh NQ, Everest P, Khoa TT, House D, Murch S, Parry C, et al. A Clinical, Microbiological, and Pathological Study of Intestinal Perforation Associated with Typhoid Fever. Clin Infect Dis [Internet]. 2004 Jul 1;39(1):61–7. Available from: https://doi.org/10.1086/421555

11. Bhan MK, Bahl R, Bhatnagar S. Typhoid and paratyphoid fever. Lancet [Internet]. 2005;366(9487):749–62. Available from: http://www.sciencedirect.com/science/article/pii/S0140673605671814

12. Levine MM, Black RE, Lanata C. Precise estimation of the numbers of chronic carriers of Salmonella typhi in Santiago, Chile, an endemic area. J Infect Dis. 1982 Dec;146(6):724–6.

13. Gonzalez-Escobedo G, Marshall JM, Gunn JS. Chronic and acute infection of the gall bladder by Salmonella Typhi: understanding the carrier state. Nat Rev Microbiol [Internet]. 2011;9(1):9–14. Available from: https://doi.org/10.1038/nrmicro2490

14. Crawford RW, Rosales-Reyes R, Ramírez-Aguilar M de la L, Chapa-Azuela O, Alpuche-Aranda C, Gunn JS. Gallstones play a significant role in Salmonella spp. gallbladder

colonization and carriage. Proc Natl Acad Sci [Internet]. 2010 Mar 2;107(9):4353 LP – 4358. Available from: http://www.pnas.org/content/107/9/4353.abstract

15. Dinbar A, Altmann G, Tulcinsky DB. The treatment of chronic biliary Salmonella carriers. Am J Med [Internet]. 1969;47(2):236–42. Available from: http://www.sciencedirect.com/science/article/pii/0002934369901491

16. Rabsch W, Tschäpe H, Bäumler AJ. Non-typhoidal salmonellosis: emerging problems. Microbes Infect [Internet]. 2001;3(3):237–47. Available from: http://www.sciencedirect.com/science/article/pii/S1286457901013752

17. Faulder KE, Simmonds K, Robinson JL. The Epidemiology of Childhood Salmonella Infections in Alberta, Canada. Foodborne Pathog Dis. 2017 Jun;14(6):364–9.

18. Majowicz SE, Musto J, Scallan E, Angulo FJ, Kirk M, O'Brien SJ, et al. The Global Burden of Nontyphoidal Salmonella Gastroenteritis. Clin Infect Dis [Internet]. 2010 Mar 15;50(6):882–9. Available from: http://dx.doi.org/10.1086/650733

19. Dhanoa A, Fatt QK. Non-typhoidal Salmonella bacteraemia: epidemiology, clinical characteristics and its' association with severe immunosuppression. Ann Clin Microbiol Antimicrob. 2009 May;8:15.

20. Graham SM, Walsh AL, Molyneux EM, Phiri AJ, Molyneux ME. Clinical presentation of non-typhoidal Salmonella bacteraemia in Malawian children. Trans R Soc Trop Med Hyg. 2000;94(3):310–4.

21. Ao TT, Feasey NA, Gordon MA, Keddy KH, Angulo FJ, Crump JA. Global burden of invasive nontyphoidal Salmonella disease, 2010(1). Emerg Infect Dis [Internet]. 2015 Jun;21(6):941–9. Available from: https://pubmed.ncbi.nlm.nih.gov/25860298

22. Uche IV, MacLennan CA, Saul A. A Systematic Review of the Incidence, Risk Factors

and Case Fatality Rates of Invasive Nontyphoidal Salmonella (iNTS) Disease in Africa (1966 to 2014). PLoS Negl Trop Dis [Internet]. 2017 Jan 5;11(1):e0005118–e0005118. Available from: https://pubmed.ncbi.nlm.nih.gov/28056035

23. Brent AJ, Oundo JO, Mwangi I, Ochola L, Lowe B, Berkley JA. Salmonella bacteremia in Kenyan children. Pediatr Infect Dis J. 2006 Mar;25(3):230–6.

24. Gordon MA. Salmonella infections in immunocompromised adults. J Infect. 2008 Jun;56(6):413–22.

25. Urdaneta V, Casadesús J. Interactions between Bacteria and Bile Salts in the Gastrointestinal and Hepatobiliary Tracts [Internet]. Vol. 4, Frontiers in Medicine . 2017. p. 163. Available from: https://www.frontiersin.org/article/10.3389/fmed.2017.00163

26. Bäumler AJ, Tsolis RM, Heffron F. Contribution of fimbrial operons to attachment to and invasion of epithelial cell lines by Salmonella typhimurium. Infect Immun [Internet]. 1996 May;64(5):1862–5. Available from: https://pubmed.ncbi.nlm.nih.gov/8613405

27. Jones BD, Ghori N, Falkow S. Salmonella typhimurium initiates murine infection by penetrating and destroying the specialized epithelial M cells of the Peyer's patches. J Exp Med [Internet]. 1994 Jul 1;180(1):15 LP – 23. Available from: http://jem.rupress.org/content/180/1/15.abstract

28. Fàbrega A, Vila J. Salmonella enterica Serovar Typhimurium Skills To Succeed in the Host : Virulence and Regulation Salmonella enterica Serovar Typhimurium Skills To Succeed in the Host : Virulence and Regulation. Clin Microbiol Rev [Internet]. 2013 Apr 1;26(2):308 LP – 341. Available from: http://cmr.asm.org/content/26/2/308.abstract

29. Vazquez-Torres A, Jones-Carson J, Bäumler AJ, Falkow S, Valdivia R, Brown W, et al.

Extraintestinal dissemination of Salmonella by CD18-expressing phagocytes. Nature [Internet]. 1999;401(6755):804–8. Available from: https://doi.org/10.1038/44593

30. Rescigno M, Urbano M, Valzasina B, Francolini M, Rotta G, Bonasio R, et al. Dendritic cells express tight junction proteins and penetrate gut epithelial monolayers to sample bacteria. Nat Immunol. 2001 Apr;2(4):361–7.

31. Hapfelmeier S, Stecher B, Barthel M, Kremer M, Müller AJ, Heikenwalder M, et al. The Salmonella Pathogenicity Island (SPI)-2 and SPI-1 Type III Secretion Systems Allow Salmonella Serovar typhimurium to Trigger Colitis via MyD88-Dependent and MyD88-Independent Mechanisms. J Immunol [Internet]. 2005 Feb 1;174(3):1675 LP – 1685. Available from: http://www.jimmunol.org/content/174/3/1675.abstract

32. Rydström A, Wick MJ. Monocyte Recruitment, Activation, and Function in the Gut-Associated Lymphoid Tissue during Oral Salmonella Infection. J Immunol [Internet]. 2007 May 1;178(9):5789 LP – 5801. Available from: http://www.jimmunol.org/content/178/9/5789.abstract

33. Sarantis H, Grinstein S. Subversion of Phagocytosis for Pathogen Survival. Cell Host Microbe [Internet]. 2012;12(4):419–31. Available from: http://www.sciencedirect.com/science/article/pii/S1931312812003083

34. Worley MJ, Nieman GS, Geddes K, Heffron F. Salmonella typhimurium disseminates within its host by manipulating the motility of infected cells. Proc Natl Acad Sci [Internet]. 2006 Nov 21;103(47):17915–20. Available from: http://www.pnas.org/cgi/doi/10.1073/pnas.0604054103

35. MIZUNO Y, TAKADA H, NOMURA A, JIN C-H, HATTORI H, IHARA K, et al. Th1

and Th1-inducing cytokines in Salmonella infection. Clin Exp Immunol [Internet]. 2003 Jan 1;131(1):111–7. Available from: https://doi.org/10.1046/j.1365-2249.2003.02060.x

36. Stoycheva M, Murdjeva M. Serum levels of interferon-γ, interleukin-12, tumour necrosis factor-α, and interleukin-10, and bacterial clearance in patients with gastroenteric Salmonella infection. Scand J Infect Dis [Internet]. 2005 Jan 1;37(1):11–4. Available from: https://doi.org/10.1080/00365540410026068

37. McCormick BA, Miller SI, Carnes D, Madara JL. Transepithelial signaling to neutrophils by salmonellae: a novel virulence mechanism for gastroenteritis. Infect Immun [Internet]. 1995 Jun 1;63(6):2302 LP – 2309. Available from: http://iai.asm.org/content/63/6/2302.abstract

38. Stecher B, Robbiani R, Walker AW, Westendorf AM, Barthel M, Kremer M, et al. Salmonella enterica Serovar Typhimurium Exploits Inflammation to Compete with the Intestinal Microbiota. PLOS Biol [Internet]. 2007 Aug 28;5(10):e244. Available from: https://doi.org/10.1371/journal.pbio.0050244

39. Mittrucker HW, Kaufmann SH. Immune response to infection with Salmonella typhimurium in mice. J Leukoc Biol. 2000 Apr;67(4):457–63.

40. Dougan G, Baker S. Salmonella enterica Serovar Typhi and the Pathogenesis of Typhoid Fever. Annu Rev Microbiol [Internet]. 2014 Sep 8;68(1):317–36. Available from: https://doi.org/10.1146/annurev-micro-091313-103739

41. Sheikh A, Khanam F, Sayeed MA, Rahman T, Pacek M, Hu Y, et al. Interferon-γ and Proliferation Responses to Salmonella enterica Serotype Typhi Proteins in Patients with S. Typhi Bacteremia in Dhaka, Bangladesh. PLoS Negl Trop Dis [Internet]. 2011 Jun 7;5(6):e1193. Available from: https://doi.org/10.1371/journal.pntd.0001193

42. Mastroeni P, Villarreal-Ramos B, Hormaeche CE. Role of T cells, TNFα and IFNγ in recall of immunity to oral challenge with virulent salmonellae in mice vaccinated with live attenuated aro− salmonella vaccines. Microb Pathog [Internet]. 1992;13(6):477–91. Available from: http://www.sciencedirect.com/science/article/pii/088240109290014F

43. Blondel CJ, Jiménez JC, Contreras I, Santiviago CA. Comparative genomic analysis uncovers 3 novel loci encoding type six secretion systems differentially distributed in Salmonella serotypes. BMC Genomics [Internet]. 2009;10(1):354. Available from: https://doi.org/10.1186/1471-2164-10-354

44. Kubori T, Matsushima Y, Nakamura D, Uralil J, Lara-Tejero M, Sukhan A, et al. Supramolecular structure of the Salmonella typhimurium type III protein secretion system. Science. 1998 Apr;280(5363):602–5.

45. LaRock DL, Chaudhary A, Miller SI. Salmonellae interactions with host processes. Nat Rev Microbiol. 2015 Apr;13(4):191–205.

46. Chen LM, Hobbie S, Galan JE. Requirement of CDC42 for Salmonella-induced cytoskeletal and nuclear responses. Science. 1996 Dec;274(5295):2115–8.

47. Zhou D, Chen LM, Hernandez L, Shears SB, Galan JE. A Salmonella inositol polyphosphatase acts in conjunction with other bacterial effectors to promote host cell actin cytoskeleton rearrangements and bacterial internalization. Mol Microbiol. 2001 Jan;39(2):248–59.

48. Fu Y, Galan JE. A salmonella protein antagonizes Rac-1 and Cdc42 to mediate host-cell recovery after bacterial invasion. Nature. 1999 Sep;401(6750):293–7.

49. Hayward RD, Koronakis V. Direct nucleation and bundling of actin by the SipC protein of invasive Salmonella. EMBO J. 1999 Sep;18(18):4926–34.

50. Zhou D, Mooseker MS, Galan JE. Role of the S. typhimurium actin-binding protein SipA in bacterial internalization. Science. 1999 Mar;283(5410):2092–5.

51. Patel JC, Galan JE. Differential activation and function of Rho GTPases during Salmonella-host cell interactions. J Cell Biol. 2006 Nov;175(3):453–63.

52. Murli S, Watson RO, Galan JE. Role of tyrosine kinases and the tyrosine phosphatase SptP in the interaction of Salmonella with host cells. Cell Microbiol. 2001 Dec;3(12):795–810.

53. Hersh D, Monack DM, Smith MR, Ghori N, Falkow S, Zychlinsky A. The Salmonella invasin SipB induces macrophage apoptosis by binding to caspase-1. Proc Natl Acad Sci U S A. 1999 Mar;96(5):2396–401.

54. Beuzon CR, Banks G, Deiwick J, Hensel M, Holden DW. pH-dependent secretion of SseB, a product of the SPI-2 type III secretion system of Salmonella typhimurium. Mol Microbiol. 1999 Aug;33(4):806–16.

55. Cirillo DM, Valdivia RH, Monack DM, Falkow S. Macrophage-dependent induction of the Salmonella pathogenicity island 2 type III secretion system and its role in intracellular survival. Mol Microbiol [Internet]. 1998 Oct 1;30(1):175–88. Available from: https://doi.org/10.1046/j.1365-2958.1998.01048.x

56. Brawn LC, Hayward RD, Koronakis V. Salmonella SPI1 effector SipA persists after entry and cooperates with a SPI2 effector to regulate phagosome maturation and intracellular replication. Cell Host Microbe [Internet]. 2007 Mar 15;1(1):63–75. Available from: https://pubmed.ncbi.nlm.nih.gov/18005682

57. Uchiya K, Barbieri MA, Funato K, Shah AH, Stahl PD, Groisman EA. A Salmonella virulence protein that inhibits cellular trafficking. EMBO J [Internet]. 1999 Jul

15;18(14):3924–33. Available from: https://pubmed.ncbi.nlm.nih.gov/10406797

58. Vazquez-Torres A, Xu Y, Jones-Carson J, Holden DW, Lucia SM, Dinauer MC, et al. Salmonella pathogenicity island 2-dependent evasion of the phagocyte NADPH oxidase. Science. 2000 Mar;287(5458):1655–8.

59. Chakravortty D, Hansen-Wester I, Hensel M. Salmonella pathogenicity island 2 mediates protection of intracellular Salmonella from reactive nitrogen intermediates. J Exp Med. 2002 May;195(9):1155–66.

60. Ruiz-Albert J, Yu X-J, Beuzon CR, Blakey AN, Galyov EE, Holden DW. Complementary activities of SseJ and SifA regulate dynamics of the Salmonella typhimurium vacuolar membrane. Mol Microbiol. 2002 May;44(3):645–61.

61. Abrahams GL, Muller P, Hensel M. Functional dissection of SseF, a type III effector protein involved in positioning the salmonella-containing vacuole. Traffic. 2006 Aug;7(8):950–65.

62. Haraga A, Miller SI. A Salmonella enterica serovar typhimurium translocated leucine-rich repeat effector protein inhibits NF-kappa B-dependent gene expression. Infect Immun. 2003 Jul;71(7):4052–8.

63. Mazurkiewicz P, Thomas J, Thompson JA, Liu M, Arbibe L, Sansonetti P, et al. SpvC is a Salmonella effector with phosphothreonine lyase activity on host mitogen-activated protein kinases. Mol Microbiol. 2008 Mar;67(6):1371–83.

64. Barthel M, Hapfelmeier S, Quintanilla-Martinez L, Kremer M, Rohde M, Hogardt M, et al. Pretreatment of mice with streptomycin provides a Salmonella enterica serovar Typhimurium colitis model that allows analysis of both pathogen and host. Infect Immun. 2003 May;71(5):2839–58.

65. Mathur R, Oh H, Zhang D, Park S-G, Seo J, Koblansky A, et al. A mouse model of Salmonella typhi infection. Cell [Internet]. 2012 Oct 26;151(3):590–602. Available from: https://pubmed.ncbi.nlm.nih.gov/23101627

66. Hormaeche CE. Natural resistance to Salmonella typhimurium in different inbred mouse strains. Immunology [Internet]. 1979 Jun;37(2):311–8. Available from: https://pubmed.ncbi.nlm.nih.gov/381178

67. Roy M-F, Malo D. Genetic regulation of host responses to Salmonella infection in mice. Genes Immun. 2002 Nov;3(7):381–93.

68. Vidal SM, Malo D, Marquis J-F, Gros P. Forward Genetic Dissection of Immunity to Infection in the Mouse. Annu Rev Immunol [Internet]. 2008 Mar 27;26(1):81–132. Available from: https://doi.org/10.1146/annurev.immunol.26.021607.090304

69. Barton CH, Whitehead SH, Blackwell JM. Nramp transfection transfers Ity/Lsh/Bcg-related pleiotropic effects on macrophage activation: influence on oxidative burst and nitric oxide pathways. Mol Med [Internet]. 1995 Mar;1(3):267–79. Available from: https://pubmed.ncbi.nlm.nih.gov/8529105

70. Fritsche G, Nairz M, Werner ER, Barton HC, Weiss G. Nramp1-functionality increases iNOS expression via repression of IL-10 formation. Eur J Immunol. 2008 Nov;38(11):3060–7.

71. Blackwell JM, Goswami T, Evans CA, Sibthorpe D, Papo N, White JK, et al. SLC11A1 (formerly NRAMP1) and disease resistance. Cell Microbiol [Internet]. 2001 Dec;3(12):773–84. Available from: https://pubmed.ncbi.nlm.nih.gov/11736990

72. Fritsche G, Dlaska M, Barton H, Theurl I, Garimorth K, Weiss G. Nramp1 functionality increases inducible nitric oxide synthase transcription via stimulation of IFN regulatory

factor 1 expression. J Immunol. 2003 Aug;171(4):1994–8.

73. Mastroeni P. Immunity to systemic Salmonella infections. Curr Mol Med. 2002 Jun;2(4):393–406.

74. Montz H, Koch KC, Zierz R, Gotze O. The role of C5a in interleukin-6 production induced by lipopolysaccharide or interleukin-1. Immunology. 1991 Nov;74(3):373–9.

75. Podack ER, Kolb WP, Muller-Eberhard HJ. The C5b-9 complex: subunit composition of the classical and alternative pathway-generated complex. J Immunol. 1976 May;116(5):1431–4.

76. Everest P, Wain J, Roberts M, Rook G, Dougan G. The molecular mechanisms of severe typhoid fever. Trends Microbiol [Internet]. 2001 Jul 1;9(7):316–20. Available from: https://doi.org/10.1016/S0966-842X(01)02067-4

77. Mastroeni P, Simmons C, Fowler R, Hormaeche CE, Dougan G. Igh-6(-/-) (B-cell-deficient) mice fail to mount solid acquired resistance to oral challenge with virulent Salmonella enterica serovar typhimurium and show impaired Th1 T-cell responses to Salmonella antigens. Infect Immun. 2000 Jan;68(1):46–53.

78. Nanton MR, Way SS, Shlomchik MJ, McSorley SJ. Cutting edge: B cells are essential for protective immunity against Salmonella independent of antibody secretion. J Immunol. 2012 Dec;189(12):5503–7.

79. Dunstan SJ, Hue NT, Han B, Li Z, Tram TTB, Sim KS, et al. Variation at HLA-DRB1 is associated with resistance to enteric fever. Vol. 46, Nature genetics. United States; 2014. p. 1333–6.

80. Dharmana E, Joosten I, Tijssen HJ, Gasem MH, Indarwidayati R, Keuter M, et al. HLA-DRB1*12 is associated with protection against complicated typhoid fever, independent of

tumour necrosis factor alpha. Eur J Immunogenet Off J Br Soc Histocompat Immunogenet. 2002 Aug;29(4):297–300.

81. Hess J, Ladel C, Miko D, Kaufmann SH. Salmonella typhimurium aroA- infection in gene-targeted immunodeficient mice: major role of CD4+ TCR-alpha beta cells and IFN-gamma in bacterial clearance independent of intracellular location. J Immunol. 1996 May;156(9):3321–6.

82. Lee S-J, Dunmire S, McSorley SJ. MHC class-I-restricted CD8 T cells play a protective role during primary Salmonella infection. Immunol Lett [Internet]. 2012/10/23. 2012 Dec 17;148(2):138–43. Available from: https://pubmed.ncbi.nlm.nih.gov/23089550

83. Pie S, Truffa-Bachi P, Pla M, Nauciel C. Th1 response in Salmonella typhimurium-infected mice with a high or low rate of bacterial clearance. Infect Immun. 1997 Nov;65(11):4509–14.

84. Fresnay S, McArthur MA, Magder L, Darton TC, Jones C, Waddington CS, et al. Salmonella Typhi-specific multifunctional CD8+ T cells play a dominant role in protection from typhoid fever in humans. J Transl Med [Internet]. 2016;14(1):62. Available from: https://doi.org/10.1186/s12967-016-0819-7

85. Gilli F, Lindberg RLP, Valentino P, Marnetto F, Malucchi S, Sala A, et al. Learning from Nature: Pregnancy Changes the Expression of Inflammation-Related Genes in Patients with Multiple Sclerosis. PLoS One [Internet]. 2010 Jan 29;5(1):e8962. Available from: https://doi.org/10.1371/journal.pone.0008962

86. Serwold T, Gonzalez F, Kim J, Jacob R, Shastri N. ERAAP customizes peptides for MHC class I molecules in the endoplasmic reticulum. Nature [Internet]. 2002;419(6906):480–3. Available from: https://doi.org/10.1038/nature01074

87. Nagarajan NA, Gonzalez F, Shastri N. Nonclassical MHC class Ib–restricted cytotoxic T cells monitor antigen processing in the endoplasmic reticulum. Nat Immunol [Internet]. 2012;13(6):579–86. Available from: https://doi.org/10.1038/ni.2282

88. Chattaragada MS, Riganti C, Sassoe M, Principe M, Santamorena MM, Roux C, et al. FAM49B, a novel regulator of mitochondrial function and integrity that suppresses tumor metastasis. Oncogene. 2018 Feb;37(6):697–709.

89. Zhang Y, Du P, Li Y, Zhu Q, Song X, Liu S, et al. TASP1 Promotes Gallbladder Cancer Cell Proliferation and Metastasis by Up-regulating FAM49B via PI3K/AKT Pathway. Int J Biol Sci. 2020;16(5):739–51.

90. Shang W, Jiang Y, Boettcher M, Ding K, Mollenauer M, Liu Z, et al. Genome-wide CRISPR screen identifies FAM49B as a key regulator of actin dynamics and T cell activation. Proc Natl Acad Sci [Internet]. 2018 Apr 24;115(17):E4051 LP-E4060. Available from: http://www.pnas.org/content/115/17/E4051.abstract

91. Chen Z, Borek D, Padrick SB, Gomez TS, Metlagel Z, Ismail AM, et al. Structure and control of the actin regulatory WAVE complex. Nature [Internet]. 2010 Nov 24;468:533. Available from: http://dx.doi.org/10.1038/nature09623

92. Fort L, Batista JM, Thomason PA, Spence HJ, Whitelaw JA, Tweedy L, et al. Fam49/CYRI interacts with Rac1 and locally suppresses protrusions. Nat Cell Biol [Internet]. 2018;20(10):1159–71. Available from: https://doi.org/10.1038/s41556-018-0198-9

93. Yuki KE, Marei H, Fiskin E, Eva MM, Gopal AA, Schwartzentruber JA, et al. CYRI/FAM49B negatively regulates RAC1-driven cytoskeletal remodelling and protects against bacterial infection. Nat Microbiol [Internet]. 2019;4(9):1516–31. Available from:

https://doi.org/10.1038/s41564-019-0484-8

94. Ullman-Culleré MH, Foltz CJ. Body condition scoring: a rapid and accurate method for assessing health status in mice. Lab Anim Sci. 1999;49:319–323.

95. Wohler JE, Barnum SR. Nylon wool purification alters the activation of T cells. Mol Immunol [Internet]. 2008/10/25. 2009 Feb;46(5):1007–10. Available from: https://www.ncbi.nlm.nih.gov/pubmed/18952296

96. Caron J, Loredo-Osti JC, Laroche L, Skamene E, Morgan K, Malo D. Identification of genetic loci controlling bacterial clearance in experimental Salmonella enteritidis infection: an unexpected role of Nramp1 (Slc11a1) in the persistence of infection in mice. Genes Immun [Internet]. 2002;3(4):196–204. Available from: https://doi.org/10.1038/sj.gene.6363850

97. Godinez I, Haneda T, Raffatellu M, George MD, Paixao TA, Rolan HG, et al. T cells help to amplify inflammatory responses induced by Salmonella enterica serotype Typhimurium in the intestinal mucosa. Infect Immun. 2008 May;76(5):2008–17.

98. Suzuki J, Denning DP, Imanishi E, Horvitz HR, Nagata S. Xk-Related Protein 8 and CED-8 Promote Phosphatidylserine Exposure in Apoptotic Cells. Science (80-) [Internet]. 2013 Jul 26;341(6144):403 LP – 406. Available from: http://science.sciencemag.org/content/341/6144/403.abstract

99. Bendall LJ, Green DR. Autopsy of a cell. Leukemia [Internet]. 2014;28(6):1341–3. Available from: https://doi.org/10.1038/leu.2014.17

100. Sprent J, Surh CD. Normal T cell homeostasis: the conversion of naive cells into memory-phenotype cells. Nat Immunol. 2011 Jun;12(6):478–84.

101. Billadeau DD, Nolz JC, Gomez TS. Regulation of T-cell activation by the cytoskeleton.

Nat Rev Immunol [Internet]. 2007;7(2):131–43. Available from: https://doi.org/10.1038/nri2021

102. Davis TA, Loos B, Engelbrecht A-M. AHNAK: the giant jack of all trades. Cell Signal. 2014 Dec;26(12):2683–93.

103. Matza D, Badou A, Kobayashi KS, Goldsmith-Pestana K, Masuda Y, Komuro A, et al. A scaffold protein, AHNAK1, is required for calcium signaling during T cell activation. Immunity. 2008 Jan;28(1):64–74.

104. Surh CD, Sprent J. Homeostasis of Naive and Memory T Cells. Immunity [Internet]. 2008;29(6):848–62. Available from: http://www.sciencedirect.com/science/article/pii/S1074761308005062

105. Sprent J, Cho J-H, Boyman O, Surh CD. T cell homeostasis. Immunol Cell Biol. 2008;86(4):312–9.

106. Cho J-H, Kim H-O, Surh CD, Sprent J. T cell receptor-dependent regulation of lipid rafts controls naive CD8+ T cell homeostasis. Immunity. 2010 Feb;32(2):214–26.

107. Zhou X, Ramachandran S, Mann M, Popkin DL. Role of lymphocytic choriomeningitis virus (LCMV) in understanding viral immunology: past, present and future. Viruses [Internet]. 2012 Oct 29;4(11):2650–69. Available from: https://pubmed.ncbi.nlm.nih.gov/23202498

APPENDIX

Appendix A: Republished agreements for figures in Chapter 1

SPRINGER NATURE LICENSE
TERMS AND CONDITIONS

Apr 23, 2020

This Agreement between Ms. Jamie Kim ("You") and Springer Nature ("Springer Nature") consists of your license details and the terms and conditions provided by Springer Nature and Copyright Clearance Center.

License Number	4815050038845
License date	Apr 23, 2020
Licensed Content Publisher	Springer Nature
Licensed Content Publication	Nature Reviews Microbiology
Licensed Content Title	Salmonellae interactions with host processes
Licensed Content Author	Doris L. LaRock et al
Licensed Content Date	Mar 9, 2015
Type of Use	Thesis/Dissertation
Requestor type	academic/university or research institute
Format	print and electronic
Portion	figures/tables/illustrations

Number of figures/tables /illustrations	1
High-res required	no
Will you be translating?	no
Circulation/distribution	50000 or greater
Author of this Springer Nature content	no
Title	Functional Characterization of Fam49b in T cells during Salmonella infection
Institution name	McGill University
Expected presentation date	Jun 2020
Portions	Supplemental figure 10
Requestor Location	Ms. Jamie Kim 9-1235 Avenue Bernard Montreal, QC H2V1V7 Canada Attn: Ms. Jamie Kim

SPRINGER NATURE LICENSE
TERMS AND CONDITIONS

Apr 23, 2020

This Agreement between Ms. Jamie Kim ("You") and Springer Nature ("Springer Nature") consists of your license details and the terms and conditions provided by Springer Nature and Copyright Clearance Center.

License Number	4815041484452
License date	Apr 23, 2020
Licensed Content Publisher	Springer Nature
Licensed Content Publication	Nature Reviews Microbiology
Licensed Content Title	Salmonellae interactions with host processes
Licensed Content Author	Doris L. LaRock et al
Licensed Content Date	Mar 9, 2015
Type of Use	Thesis/Dissertation
Requestor type	academic/university or research institute
Format	print and electronic
Portion	figures/tables/illustrations

Number of figures/tables /illustrations	1
High-res required	no
Will you be translating?	no
Circulation/distribution	50000 or greater
Author of this Springer Nature content	no
Title	Functional Characterization of Fam49b in T cells during Salmonella infection
Institution name	McGill University
Expected presentation date	Jun 2020
Portions	Figure 1
Requestor Location	Ms. Jamie Kim 9-1235 Avenue Bernard Montreal, QC H2V1V7 Canada Attn: Ms. Jamie Kim

Appendix B: Animal Protocol Certificate

McGill

October 10, 2019

Animal Certificate

This is to certify that **Dr. Danielle Malo, Department of Medicine,** currently holds an approved Animal Use Protocol **# 2009-5797** with McGill University and its Affiliated Hospitals' Research Institutes for the following project:

Animal Use Protocol Title: Functional characterization of new mouse models for susceptibility to Salmonella infection identified in a genome-wide ENU mutagenesis screen / A syst-OMICS approach to ensuring food safety and reducing economic burden of salmonellosis / Analysing the dual function of a novel nuclear receptor coactivator in the CNS / Oxford-Brain@McGill -ZNZ neuroscience collaboration

Start date: October 1, 2019

Expiration date: October 1, 2020

McGill University and Affiliated Hospitals Research Institutes recognize the importance of animal research in our efforts to further our knowledge of natural processes, diseases and conservation. Research, educational and testing projects are conducted with full commitment to the wellbeing of the animal subjects. In order to limit animal use to meritorious research or educational projects, the institution relies on stringent peer review processes, along with assessment of ethical issues by the Animal Care Committee. McGill University recognizes that the use of animals in research, teaching and testing carries significant responsibilities. The institution will continue to develop and maintain guidelines and regulations, following the high standards established by the Canadian Council on Animal Care. It is committed to conducting the highest-quality research and to providing animals with the best care.

Melanie Tremblay, Ph.D
Animal Ethics and Compliance Admin | Animal Compliance Office
Office of Vice-Principal (Research and Innovation)
Suite 325, James Administration Building, McGill University
845 Sherbrooke Street West, Montreal, Quebec, Canada H3A 0G4
animal.approvals@mcgill.ca